AD610465

MAGNETIC HYSTERESIS DAMPING
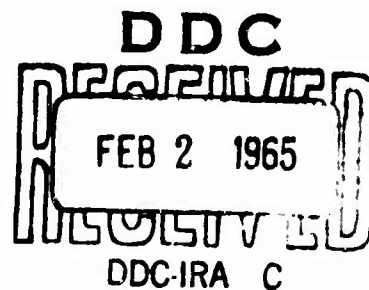
OF

SATELLITE ATTITUDE MOTION

FINAL REPORT

VOLUME I

16 NOVEMBER 1964

COPY 2 OF 3 R

HARD COPY $. 3.00

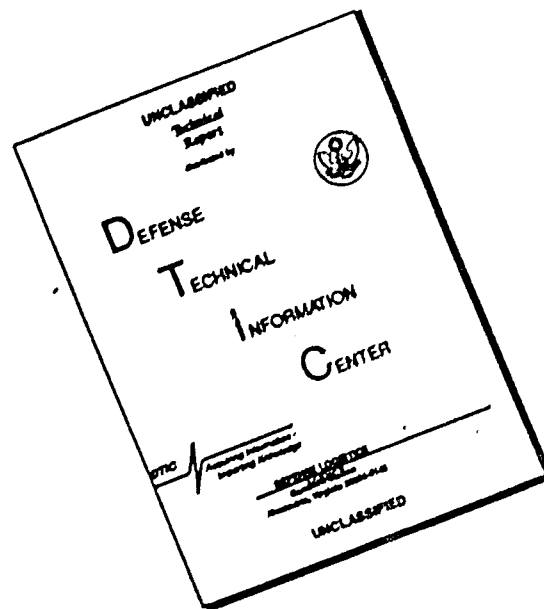MICROFICHE $. 0.75

75P

Prepared Under
Contract No. N178-8450
for

U.S. Naval Weapons Laboratory

Dahlgren, Virginia

DDC

FEB 2 1965

DDC-IRA C

GENERAL ELECTRIC

SPACECRAFT DEPARTMENT

DISCLAIMER NOTICE

THIS DOCUMENT IS BEST
QUALITY AVAILABLE. THE COPY
FURNISHED TO DTIC CONTAINED
A SIGNIFICANT NUMBER OF
PAGES WHICH DO NOT
REPRODUCE LEGIBLY.

MAGNETIC HYSTERESIS DAMPING

OF

SATELLITE ATTITUDE MOTION

FINAL REPORT

VOLUME I

16 NOVEMBER 1964

Prepared Under
Contract No. N178-8450
for

U.S. Naval Weapons Laboratory

Dahlgren, Virginia

GENERAL ELECTRIC

SPACECRAFT DEPARTMENT

ABSTRACT

The attitude dynamics of a gravity-gradient oriented satellite, which employs soft nickel-iron rods as magnetic hysteresis dampers, is simulated by a digital computer program. A subroutine was generated to compute the flux induced in the rods for an arbitrary vehicle orientation relative to the earth's magnetic field vector. This subroutine was added to an existing computer program. Analytical expressions were fitted to empirical major and minor hysteresis loops, and a logic scheme was devised for tracing BH curves with an arbitrarily fluctuating applied amgnetic field. This enables simulation of the effects due to the magnetic field encountered in orbit. Volume I of this report describes the analysis and the computer program in detail. Volume II presents the results of computer runs made under various initial conditions.

TABLE OF CONTENTS

SECTION 1.

INTRODUCTION

The U.S. Naval Weapons Laboratory at Dahlgren, Va., awarded the Spacecraft Department of the General Electric Co. a contract for performing the digital simulation of the attitude dynamics of a gravity-gradient oriented satellite employing soft nickel-iron rods as magnetic hysteresis dampers. The work, performed under Contract No. N178-8450 as amended by Contract Change Notice, consisted of (1) obtaining test data for the rod material from the Allegheny Ludlum Steel Corporation; (2) fitting analytical expressions to these magnetic curves; (3) generating a magnetic torque subroutine for incorporation into an existing GE digital program for simulating the attitude dynamics of the satellite; and (4) making computer runs with various initial conditions and vehicle parameters, as specified by NWL.

The report on this contract is submitted in two volumes. Volume I includes a summary of the work done, explains the magnetics fundamentals involved, and describes the approaches taken to solve the problems. A complete description of the hysteresis torque subroutine is presented, including the logical rules, the scheme for implementing the logic, and the complete equations. The unsuccessful approaches are also described briefly.

Volume II includes a brief description of the satellite in terms of the characteristics and parameters which affect its attitude performance, a list of the initial and other conditions for the various computer runs, and the results of these runs.

The Allegheny Ludlum data used is for the same material as that in the hysteresis rods in the satellite. However, the heat treatment of the satellite rods is slightly different from that of the sample used for taking the data. Also, the maximum value of the earth's magnetic field encountered in orbit is somewhat greater than the maximum value used in taking the data. The data were therefore extrapolated to provide the required range. Additional data, taken with greater field strengths applied to samples having appropriate heat treatment, have been requested from Allegheny Ludlum, but have not yet been received. When they are received, these curves can be compared with those used in the digital simulation.

SECTION 2.

SUMMARY

The work reported herein includes (1) determining the general requirements of the hysteresis torque subroutine, in terms of the representation of the magnetic curves and their use in conjunction with a logic scheme in a manner which is compatible with the digital computer; (2) fitting analytical expressions to the original magnetic data, after making the corrections for the demagnetization factor of the rods; and (3) devising a scheme for using these expressions, together with a minimum amount of information about the past history of each rod, to derive magnetic curves under the conditions associated with an arbitrarily varying applied magnetic field.

The magnetics and dynamics fundamentals which bear on the problem are discussed. It is shown that a continuously varying magnetic field applied to a hysteresis material causes a continuously varying torque which is non-conservative around a cycle because of the hysteresis losses.

The digital computer program which simulates the satellite attitude dynamics, and to which the magnetic hysteresis torque subroutine is added, is briefly described in terms of its flexibilities, limitations, and capabilities applicable to the present contract.

The various approaches used to derive analytical expressions to fit the magnetic curves are described. Various methods had varying degrees of success. The reason for abandoning each of the unsuccessful methods is given.

The work done demonstrates that the flux density in a ferromagnetic rod subjected to an arbitrarily varying magnetic field can be calculated by a digital computer. The limited core storage and running time economy dictate simplifications in the representation of the magnetic curves. A set of ten polynominals was used to represent the original data. In the program, other curves are interpolated between these polynomials. An interpolation coefficient which varies with the applied field is employed to meet the various conditions imposed on the interpolated curves. From these curves, the flux density in each rod is computed at every integration interval. These values are then used to compute the instantaneous magnetic moments and hysteresis torques.

The computation of other torques, calculation of vehicle characteristics from input data, integration of the equations of attitude motion with respect to time, and other required computations are performed by the existing digital program.

SECTION 3.

MAGNETICS FUNDAMENTALS

3.1 FERROMAGNETIC MATERIALS AND HYSTERESIS LOOPS

When a ferromagnetic material is placed in a magnetic field, there will be induced in the material a flux density which is a function of the magnitude of the magnetic field and the magnetic characteristics of the material. This can be expressed as

$$B_i = H_i + 4\pi I_i \tag{1}$$

where

B_i = internal magnetic flux density

H_i = internal magnetic intensity

I_i = internal intensity of magnetization

and

$$I_i = K H_i \tag{2}$$

where

K = magnetic susceptibility.

If the permeability of the material is defined as

$$\mu = 1 + 4\pi K \tag{3}$$

$$B_i = \mu H_i \tag{4}$$

In a ferromagnetic material the permeability is not a constant but is a function of B_i or H_i.

As H_i is varied from $(H_i)_{max}$ to $(H_i)_{min}$, B_i will vary from a maximum to a minimum value in a manner described as a hysteresis loop, such as the outer loop in Figure 3-1. The coordinates of the tips of such a loop are designated $\pm H_{i\,(max)}$ and $\pm B_{(max)}$.

If while traversing the hysteresis loop from $(H_i)_{max}$ to $-(H_i)_{min}$, the magnitude of the applied field H_i is reversed, a minor hysteresis loop is formed. The characteristics of this minor hysteresis loop are functions of the point of flux reversal. Further flux reversals will produce additional minor hysteresis loops. Once the major hysteresis loop has been traversed and a field reversal takes place, the loop being formed will bend towards the point of last reversal. Internal reversals within a minor hysteresis loop will follow this property of bending towards the point of last reversal.

The magnetic characteristics of any material are a function of the magnetic field intensity internal to the material. In a rod, poles are induced at the ends of the rod which are opposite to that of the applied field. This is a demagnetizing field and its effect is to reduce the internal field in the rod; it is a function of the length to diameter ratio of the rod.

$$H_i = H_o - NI \tag{5}$$

where

H_i = internal field
H_O = external field
N = demagnetizing factor
I = intensity of magnetization

Since

$$B_i = H_i + 4\pi I, \tag{6}$$

$$I = \frac{B_i - H_i}{4\pi} \tag{7}$$

and

$$H_i = H_O - \frac{N}{4\pi}(B_i - H_i) \tag{8}$$

Since $\quad H \ll B_i$

$$H_i = H_O - \frac{N}{4\pi}B_i \tag{9}$$

Values of $\frac{N}{4\pi}$ are given as a function of $\frac{\ell}{d}$ and the material permeability in Borzorth, "Ferromagnetism" pp. 846-847. For a long cylinder with infinite permeability

$$\left(\frac{N}{4\pi}\right) = \frac{4.62 \log_{10}\left(\frac{\ell}{d}\right) - .92}{2\left(\frac{\ell}{d}\right)^2} \tag{10}$$

The magnetic moment, M, of a bar is

$$M = m\ell \tag{11}$$

where

m = pole strength
ℓ = pole separation

Since

$$m = \frac{\phi}{4\pi} = \frac{AB}{4\pi},$$

$$M = \frac{VB}{4\pi} \tag{12}$$

However, due to leakage and saturation effects, the pole separation is not always equal to the length of the bar. Borzorth and Chapin* show that the pole separation is approximately .73 the length of the bar. Therefore

$$M = .73\frac{VB}{4\pi} \tag{13}$$

---

*Bozorth and Chapin, "Demagnetizing Factors of Rods," Journal of Applied Physics, Vol. 13, p. 320, May, 1942.

The Barkhausen effect describes the irregularities in the magnetization of a ferromagnetic material. The magnetization does not take place instantaneously but in steps as the field strength is varied. As $\frac{dH}{dt}$ approaches zero, $\frac{dB}{dH}$ approaches the total change in magnetization for high nickel alloys (~80% N_i, 20% Fe). Investigation and consultation with Allegheny Ludlum indicates that this should not be a problem in 4750 Nickel Iron.

It is assumed that the rods are separated enough so that there is not magnetic interaction between them. Thus each rod acts as though it is alone in the magnetic environment.

The rod material used was AEM 4750 (Allegheny Electrical Metal) which is a nickel iron alloy containing approximately 48% nickel, the remainder being iron. In order to obtain optimum magnetic characteristics the material must be annealed. It should be noted that the anneal recommended by Allegheny Ludlum was not that used by the Applied Physics Laboratory for the rods. A comparison is given as follows:

	Allegheny Ludlum	APL
Heat Treatment	$2150^{O}F$	$1650^{O}F$ to $1740^{O}F$
Cooling Rate	$100^{O}F$ per hour max. to $1100^{O}F$	$54^{O} \pm 18^{O}F$ per hour from $1100^{O}F$ to $570^{O}F$

The exact effect of this variation of heat treatment is unknown; however, it is thought that the APL heat treatment might produce greater hysteresis loss than the Allegheny Ludlum.

3.1.1 Test Data

There is no way to predict the magnetic properties of ferromagnetic materials from any fundamental properties of the material. The newest approach has been the work of Rayleigh which only applies to unsaturated regions of low flux density. The only method for obtaining reliable data is by test procedures.

Allegheny Ludlum ran hysteresis loops on a ring sample of AEM 4750, annealed to produce optimum magnetic characteristics; i.e., 2150OF anneal. Curves were run for B_{max} = $\pm$ 2000, $\pm$ 4000, $\pm$ 6000 and $\pm$ 8000 gauss, showing major and minor hysteresis loops. These curves are given in Figures 3-1, 3-2, 3-3 and 3-4.

The curves were obtained from a demagnetized sample, first obtaining the major hysteresis loop and then the minor hysteresis loops. The slight shifting of the loops is a result of instability in the test equipment rather than inherent magnetic properties.

3.2 CONVERSION OF MECHANICAL ENERGY TO HEAT THROUGH MAGNETIC HYSTERESIS LOSS

It has been demonstrated that the torque acting on a ferromagnetic rod placed in the earth's magnetic field is associated with a change in the mechanical energy equal and opposite to the change in the magnetic energy stored in the rod.
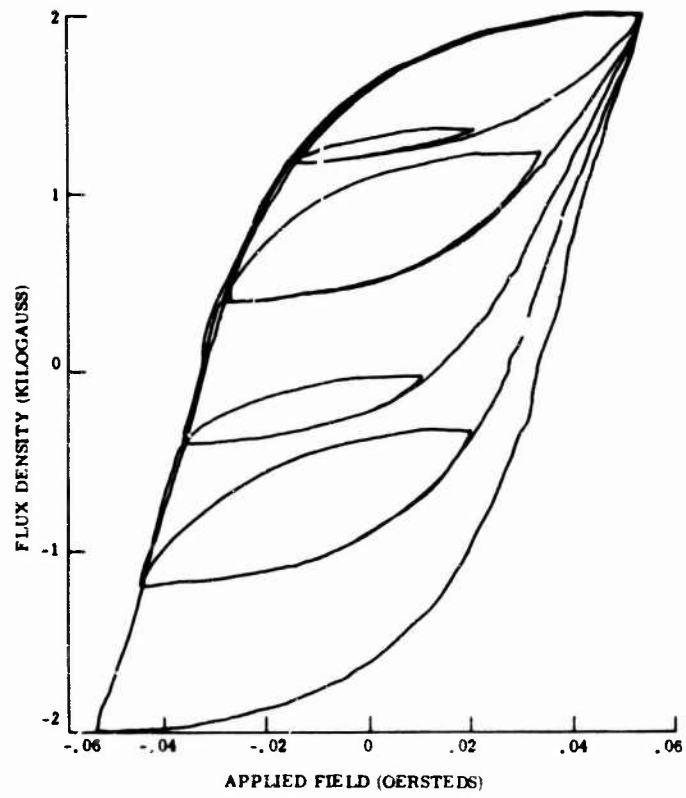
Figure 3-1. Allegheny-Ludlum 2 - Kilogauss Data
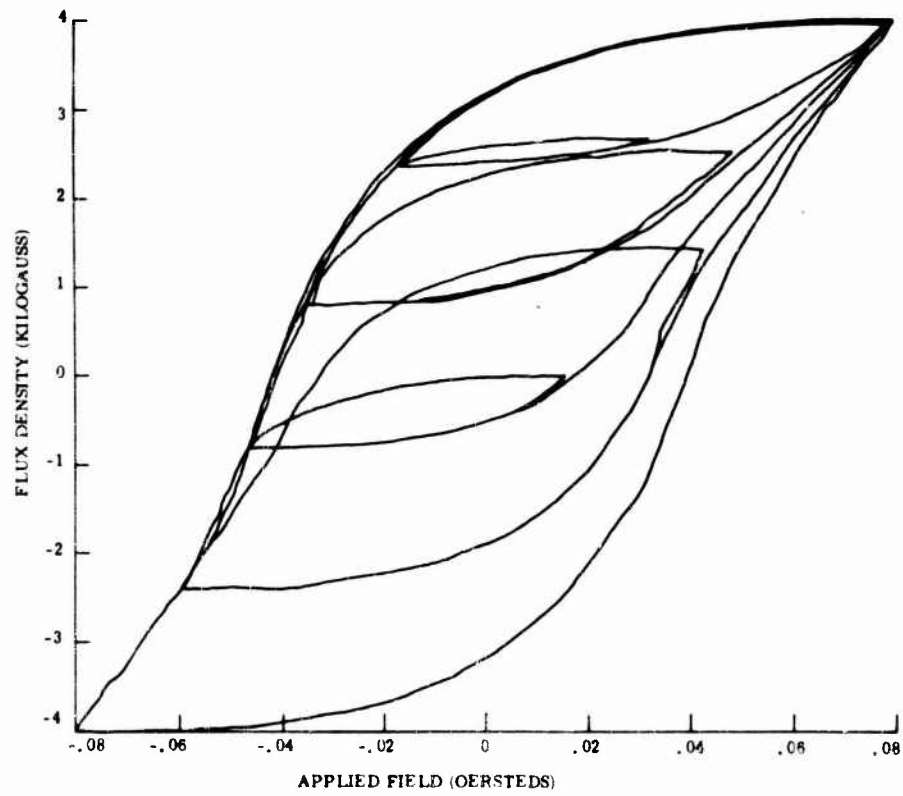
Figure 3-2. Allegheny-Ludlum 4 - Kilogauss Data

3-4
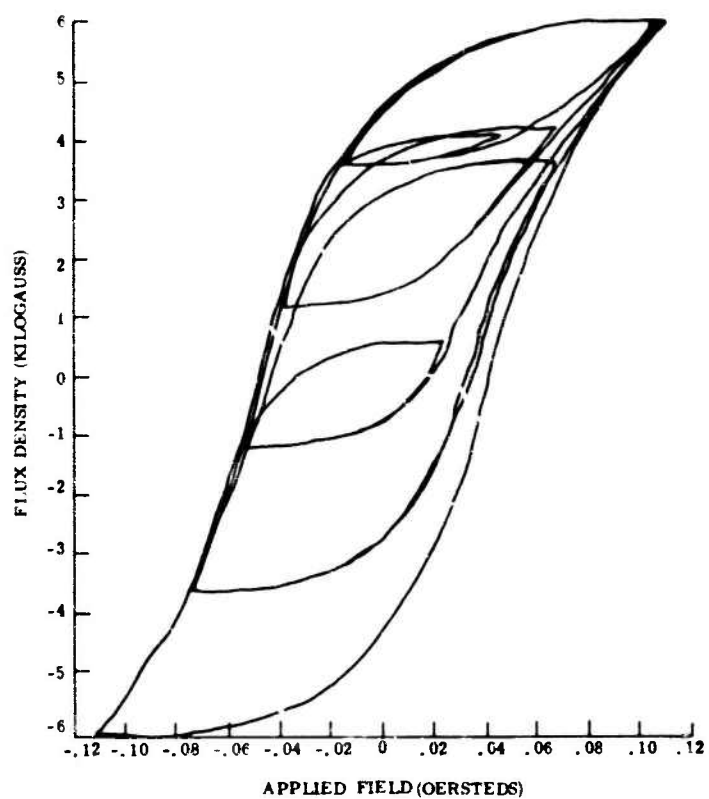
Figure 3-3. Allegheny-Ludlum 6-Kilogauss Data
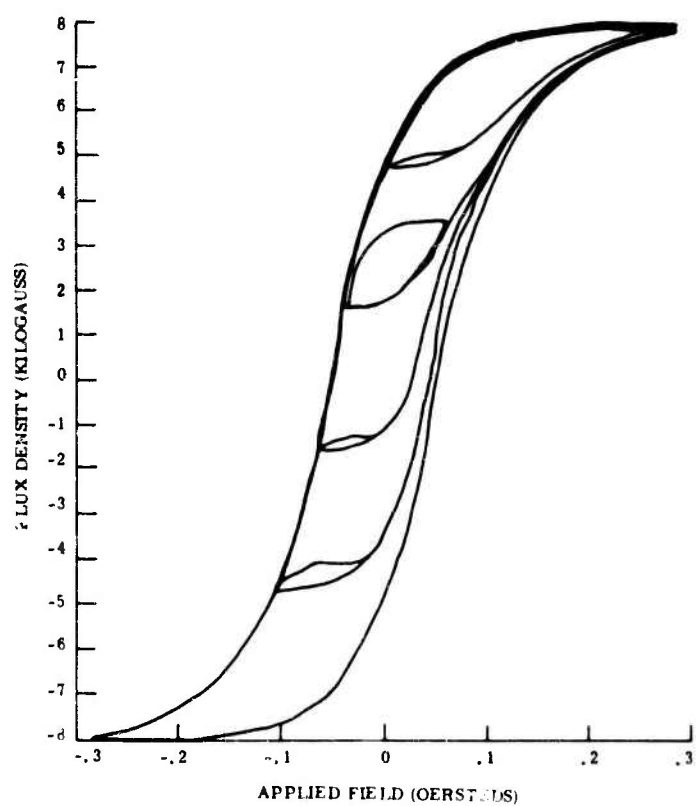
Figure 3-4. Allegheny-Ludlum 8-Kilogauss Data

Figure 3-5 shows such a rod placed in the earth's field, which has the value H_E. The component of the field along the rod is

$$H_A = H_E \cos \theta \tag{1}$$
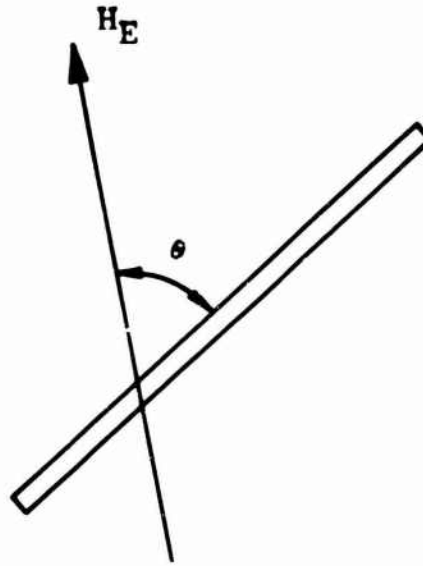
Figure 3-5. Ferromagnetic Rod in the Earth's Field

This is the only component which is effective in producing any flux, ϕ, in the rod. The differential flux crossing the differential area, dA, at some point, is the flux density, B, multiplied by the area,

$$d\phi = BdA. \tag{2}$$

The flux density is

$$B = \mu H_I = \mu(H_A - D_M E), \tag{3}$$

where H_I is the internal (induced) field, μ is the true permeability of the rod material, and D_M is the demagnetization factor.

The elementary volume of length $d\ell$ is

$$dV = d A \, d\ell \tag{4}$$

The differential magnetic moment of dV is

$$dM = \frac{1}{4\pi} \, d\phi \, d\ell$$

$$= \frac{1}{4\pi} \, B \, d A \, d\ell$$

$$= \frac{1}{4\pi} \, B \, dV. \tag{5}$$

The total magnetic moment of the rod is the integral of this expression throughout the volume, V,

$$M = \frac{1}{4\pi} \int_V B \, dV. \tag{6}$$

The torque on the rod is

$$T = M H_E \sin \theta.$$

$$= \frac{1}{4\pi} H_E \sin \theta \int_V B \, dV. \tag{7}$$

If the rod rotates through an angle $d\theta$ under the influence of this torque, the mechanical energy is

$$dW = T \, d\theta$$

$$= \frac{1}{4\pi} H_E \sin \theta \, d\theta \int_V B \, dV. \tag{8}$$

The rotation will also produce a differential change in the applied field,

$$d H_A = -H_E \sin \theta \, d\theta. \tag{9}$$

The corresponding change in the magnetic energy, E, per unit volume, is

$$\frac{d^2 E}{dV} = \frac{1}{4\pi} B \, d H_A. \tag{10}$$

The change in the magnetic energy of the whole rod is the volume integral of this, or

$$d E = \frac{1}{4\pi} d H_A \int_V B \, dV. \tag{11}$$

Equation (9) is substituted into (11)

$$d E = - \frac{1}{4\pi} H_E \sin \theta \, d\theta \int_V B \, dV. \tag{12}$$

From equations (8) and (12),

$$dW + dE = 0. \tag{13}$$

This shows that the mechanical energy gained is equal to the magnetic energy lost, and vice versa. The equation and its method of derivation also show that the exchange of energy is continuous, because it takes place with differential motions. It is not necessary to traverse a complete magnetic hysteresis loop, nor any specified fraction of it, for the energy exchange to take place. Therefore, mechanical energy is continually converted into heat through hysteresis losses as the motion causes traversal of the hysteresis curves.

3.3 COMPUTATION OF MAGNETIC HYSTERESIS TORQUES

The results of the previous sections are used to derive the torque expressions used in the program and the numerical value of the conversion factor.

Equation (13) of Section 3.1 relates the magnetic moment of one rod to the flux density at its center. The factor .73 accounts for the decrease of flux toward the ends of the rod. That is,

$$\int_V B \, dV = .73 \, BV. \tag{1}$$

Each of the rods used is 60 inches long and .11 inches in diameter. The volume is $2.974\,\pi$ cubic centimeters. The ratio of the magnetic moment to the flux density at the center of the rod is therefore .5428 dyne-centimeters per oersted-gauss. This number is doubled for two rods (with negligible proximity effect), and converted to the units used in the program. Ti.~ value is then 80.067×10^{-6} foot-pounds per oersted-kilogauss. This factor is designated H_{DC} and is an input constant in the program. In general, this factor accounts for the rod length, rod diameter, decrease of flux toward the ends of the rod, number of rods, proximity effect, and units conversion factors.

The torque on an elementary volume, dV, of the rod is

$$dT = I \times H_E \, dV, \tag{2}$$

where I is the intensity of the magnetization in the rod, and H_E is the applied magnetic field, undisturbed by the rod. The magnetic moment of the elementary volume is

$$d M = I \, dV. \tag{3}$$

Using the expression for I from equation (7) of Section 3.1, with H_i negligible in comparison with B_i, and equation (2) above, in (3), leads to

$$d M = \frac{B_i}{4\pi} \, dV, \tag{4}$$

and

$$d T = \frac{B_i}{4\pi} \times H_E \, dV$$

$$= d M \times H_E. \tag{5}$$

The torque on the whole rod is

$$T = M \times H_E. \tag{6}$$

This is consistent with equations (5), (6), and (7) of Section 3.2 where the value of the vol..ne integral is given by equation (1) above.

SECTION 4.
DIGITAL COMPUTER SIMULATION

The attitude dynamical equations of the satellite were simulated by an IBM 7094 computer program (GOLD-N-ROD), coded in Fortran II. This was accomplished by adding a magnetic hysteresis torque subroutine to the existing program. This program is described in detail in Reference 1. The torque subroutines not needed for this simulation were deleted from the program.

The applicable portions of the GOLD-N-ROD program are described below, in sufficient detail to enable an understanding of those capabilities and limitations which affect this simulation.

The magnetic hysteresis torque subroutine is described in complete detail. This includes the magnetic curves for the material, the fitting of analytical expressions to these curves, the logic for tracing BH curves with an arbitrarily varying H, and the equations which constitute the magnetic hysteresis torque subroutine.

4.1 GENERAL DESCRIPTION OF THE DIGITAL COMPUTER PROGRAM

The program is an IBM 7094 digital simulation of the attitude dynamics of a passively oriented satellite. The differential equations describing the attitude motion are numerically integrated with respect to orbit angle (in lieu of time). This program was developed prior to the NWL contract. The various features, capabilities, and limitations of the program are best described in connection with the various subroutines.

4.1.1 Input Subroutine (INPUT)

For convenience, the various inputs are grouped in sets as described below.

    a.   Card 1 - This is the title card, and may contain any 72 alphanumeric characters.

    b.   Set 1. Earth Constants - At present, only the solar pressure and solar heat flux constants are listed as inputs. This is done in order to be able to include or exclude the effects of solar torque or thermal bending as desired.

          All of the other constants are internal to the program. These include the angle between the ecliptic and equatorial planes, the product of the universal gravity constant and earth's mass, the earth's orbital angular rate, the earth's spin rate, and the earth's equatorial and polar radii. The earth's orbital angular rate is a constant, because the earth is assumed to be in a circular orbit about the sun. The constants in the program are in the foot-pound-second system and must be changed if a different system of units is employed.

    c.   Set 2. Satellite Orbital Parameters - These include the geocentric distances at apogee and perigee; the precession rate and inclination of the orbit plane, and the initial values of the right ascension of the ascending node; the time of year, Greenwich mean time; and the orbital angular relations between the ascending node, perigee, and the satellite's position at injection.

d. Set 3. Characteristics of the Central Body - These include the radius of the body (assumed spherical), its mass, moments of inertia, and the diffuse reflectance of its surface.

e. Set 5. Characteristics of the Rod and Tip Mass - The characteristics of the rod include its length, radius, mass density per unit length, thickness of wall, thermal conductivity, linear coefficient of thermal expansion, and the absorptance of its surface.

   The characteristics of the tip mass include its radius (the mass is assumed to be spherical), the diffuse reflectance of its surface, and its mass.

f. Set 7. Initial Conditions - These are the initial values of the three Euler angles which relate the body reference frame to the orbital reference frame, and the three body-axis rates.

g. Set 8. Integration Parameters, Time and Print Controls - These include the tolerable errors associated with the numerical integration, initial step size, print-out interval, and stop time. All of these are more fully explained in the section on numerical integration.

4.1.2 Initialization Subroutines (INITIA and VCINIT)

Certain parameters which are varied from one run to another are constant for a particular run, and are therefore initialized for economy. These include orbital parameters, elements of direction cosine matrixes involving fixed angles, and vehicle characteristics. The vehicle characteristics include the mass, mass moments, and moments of inertia of the straight rod and certain combinations of parameters which are recurrent in the solar-torque equations.

4.1.3 Orbital Subroutine (ORBIT)

The center of mass of the satellite is assumed to trace a circular or elliptical path about the geocenter. The inclination of the orbit plane with respect to the equatorial plane is constant, but provision is made for a constant rate of precession of the line of nodes.

The outputs of this subroutine are time, satellite orbital angle and geocentric distance, certain time derivatives of these quantities, altitude above the earth's surface, earth's orbital position, and a parameter used for the earth's shadow criterion.

4.1.4 Matrix Subroutine (MATRIX)

This subroutine calculates elements of the direction cosine matrixes, certain of their time derivatives, and the satellite's latitude and longitude.

4.1.5 Earth's Shadow Criterion

The sun's rays are considered to be parallel, and therefore the earth's shadow is assumed to be a sharply defined cylinder. When the satellite is in the earth's shadow, all of the solar effects are zero.

4.1.6 Rod Geometry Subroutine (RODN)

This subroutine is used only when the satellite is not in the earth's shadow. It includes the equations which describe the thermally bent rods under the various conditions of full, partial, or no illumination. The length of rod illuminated is dependent upon the shadow cast by the (spherical) central body, unless the whole satellite is in the earth's shadow. The mass moments of the bent rod are computed.

4.1.7 Center of Mass Subroutine (CMASS)

The instantaneous moments and the coordinates of the instantaneous center of mass of the entire satellite are computed. The vector distances from this center of mass to the base and tip of each rod are computed. Time derivatives of certain of the foregoing variables are also computed.

4.1.8 Moments of Inertia Subroutine (MOMIN)

The instantaneous moments and products of inertia of the rod and of the entire satellite, and their time derivatives, are computed for the current condition of rod illumination.

4.1.9 Solar Torque Subroutine (SOLTOR)

This subroutine is used only when the satellite is not in the earth's shadow. The solar radiation pressure torques on the central body, rod, and tip mass are computed. The sun's rays are all considered parallel.

4.1.10 Magnetic Hysteresis Torque Subroutine (HYSTOR)

This subroutine is discussed in detail in section 4.2.

4.1.11 Gravity Gradient Torque Subroutine (GRATOR)

This subroutine computes the gravity gradient torques on the satellite from its moments and products of inertia. The earth's gravitational field is assumed to follow an inverse square law.

4.1.12 Derivative Subroutine (DERIV)

The various torques are added to obtain the total torques acting on the satellite. Euler's dynamical equations are solved explicitly (in matrix form) to obtain the body-axis angular accelerations. The Euler angular rates are computed from the Euler angles and the body-axis rates. Each time derivate is converted to the corresponding derivative with respect to orbital angle, by dividing by the orbital angular rate.

4.1.13 Numerical Integration Subroutine (NOL3)

The Adams-Moulton method of numerical integration is used. A variable integration interval is used. Specified error criteria are applied to the estimated numerical integration error for each variable to determine whether the interval is satisfactory. If the interval is satisfactory with respect to every integrated variable, the results of the integration are accepted by the program. If the interval is unsatisfactory, it is halved until a satisfactory interval is obtained. Whenever a specified number of consecutive satisfactory intervals have been obtained, the interval is tentatively doubled. The results of using the new interval are tested against the error criteria as explained above.

4.1.14 Output Subroutine (OUTPUT)

This subroutine computes any variables desired as output which have not been previously computed in other subroutines. Usually, the output time intervals are much larger than the integration intervals, and so the output computations are performed only at those intervals when output is required. However, because of the requirement for sometimes plotting the BH curves, more frequent outputs are desirable for the magnetic hysteresis program. Therefore, output is obtained at every good integration step.

The output variables required, which are not available from other subroutines, include the classical Euler angles, θ_1, θ_2, and θ_3, one Euler angular rate, $\dot{\theta}_3$, and the three inertial coordinates, X, Y, and Z, of the satellite position.

The Euler angles depend upon the values of certain $[E]$ matrix elements.

$$\sin \theta_2 = \sqrt{1 - E_{11}^2} \ . \tag{1}$$

If this quantity is equal to or less than 0.001, it is considered to be essentially zero. This yields the singular case, and the computation and printout of θ_1, θ_2, and θ_3 are omitted for that time interval. If the quantity is greater than 0.001, the computations proceed.

$$\theta_2 = \cos^{-1}(E_{11}) \ . \tag{2}$$

The computer subroutine used for the inverse cosine automatically puts the angle in the first or second quadrant. θ_1 is computed next.

If $E_{13} \stackrel{<}{=} 0$,

$$\theta_1 = \sin^{-1}\left(\frac{E_{12}}{\sin \theta_2}\right) \ . \tag{3}$$

The computer subroutine used for the inverse sine automatically puts the angle in the first or fourth quadrant.

If $E_{13} > 0$, and if $E_{12} \geqq 0$,

$$\theta_1 = 180^o - \sin^{-1}\left(\frac{E_{12}}{\sin\theta_2}\right). \tag{4}$$

If $E_{13} > 0$, and if $E_{12} < 0$,

$$\theta_1 = -180^o - \sin^{-1}\left(\frac{E_{12}}{\sin\theta_2}\right). \tag{5}$$

θ_3 is computed next.

If $E_{31} \geqq = 0$,

$$\theta_3 = \sin^{-1}\left(\frac{E_{21}}{\sin\theta_2}\right). \tag{6}$$

If $E_{31} < 0$, and if $E_{21} \geqq 0$,

$$\theta_3 = 180^o - \sin^{-1}\left(\frac{E_{21}}{\sin\theta_2}\right). \tag{7}$$

If $E_{31} < 0$, and if $E_{21} < 0$,

$$\theta_3 = -180^o - \sin^{-1}\left(\frac{E_{21}}{\sin\theta_2}\right). \tag{8}$$

The angular rate $\dot{\theta}_3$ is

$$\dot{\theta}_3 = \omega_{X1} - \frac{1}{\sin^2\theta_2}\left[E_{11}\left(E_{21}\,\omega_{Y1} + E_{31}\,\omega_{Z1}\right) + E_{13}\,\dot{\eta}\right], \tag{9}$$

where $\dot{\eta}$ is the orbital angular velocity, and ω_{X1}, ω_{Y1}, and ω_{Z1} are the body axis rates relative to an inertial frame.

The inertial coordinates of the satellite are expressed in kilometers,

$$X = -0.3048 \times 10^{-3}\, A_{11}\, R_A, \tag{10}$$
$$Y = -0.3048 \times 10^{-3}\, A_{12}\, R_A, \tag{11}$$
$$Z = 0.3048 \times 10^{-3}\, A_{13}\, R_A, \tag{12}$$

where R_A is the geocentric altitude of the satellite in feet, and A_{11}, A_{12}, and A_{13} are elements of the direction cosine matrix relating the orbital and inertial reference frames.

4.2 MAGNETIC HYSTERESIS TORQUE SUBROUTINE (HYSTOR)

This subroutine computes the instantaneous torque on the satellite due to the action of the earth's magnetic field on the hysteresis rods.   .e torque depends upon the magnetic moments of the rods, which in turn depend upon their magnetic flux densities. The major requirement of this subroutine is therefore the tracing of BH curves, or the determination of flux density under the condition of a fluctuating applied field. The fluctuations are slow, so time rates of change are negligible.

4.2.1 Organization and Logic of the Subroutine

The subroutine first computes the components of the earth's magnetic field in the orbital (local vertical) reference frame. This is done by the use of a program obtained from the Armed Forces Special Weapons Command at Kirtland Air Force Base, New Mexico. These field components are transformed into the satellite body reference frame.

The hysteresis rods lie along the Y and Z geometric axes of the satellite main body. The same logic and equations are used for each of these axes. Therefore, the explanation which follows applies to each.

Three basic rules are used in tracing the BH curves, using an arbitrarily fluctuating applied magnetic field, H.

First, it is assumed that the initial path is the major hysteresis loop whose end points correspond to the maximum values of the earth's magnetic field encountered at the perigee altitude. Such a loop is illustrated in Figure 4-1, with end points A and B. The assumption is justified on the grounds that the satellite will undoubtedly experience this value of applied field during its history of assembly, test, and launch.

Second, whenever a reversal in the algebraic sign of the field increment (equivalent to a reversal in the sign of H) occurs, the new BH curve must pass through the last prior reversal point. In Figure 4-1, a reversal occurs at point C, and the curve CD, if extended, would pass through point B. Similarly, the curve DE, if extended, would pass through point C, etc. Thus the end point of any curve is the beginning point of the previous curve. This rule is based on the known effect of applying an alternating field superimposed on a direct field. That is, a minor loop between the same two end points is traced repetitively. In the case of a rapidly alternating field, several cycles might be required before the loop becomes exactly repetitive. However, it is believed that with slow variations in the applied field, the first traverse of the loop very closely approximates what would become the final path. It should be noted that there is no implication here that a complete minor loop is actually traced, but only that the path of the BH point is along a curve which passes through the prior reversal point. Of course, if the variation in H is great enough, that point will be reached, in which case the complete minor loop will have been traced once.

Third, whenever the value of H ranges beyond the end point of the present curve (the prior reversal point discussed above), the path reverts to the previous curve of like kind (that is the previous ascending or descending curve). For example, if the BH point is on curve FE of Figure 4-1, and H subsequently increases beyond E, the curve DC will then be followed. This rule may not be strictly correct, but it is the consensus of expert opinion that it is a good approximation, and as good as can be done with available knowledge.
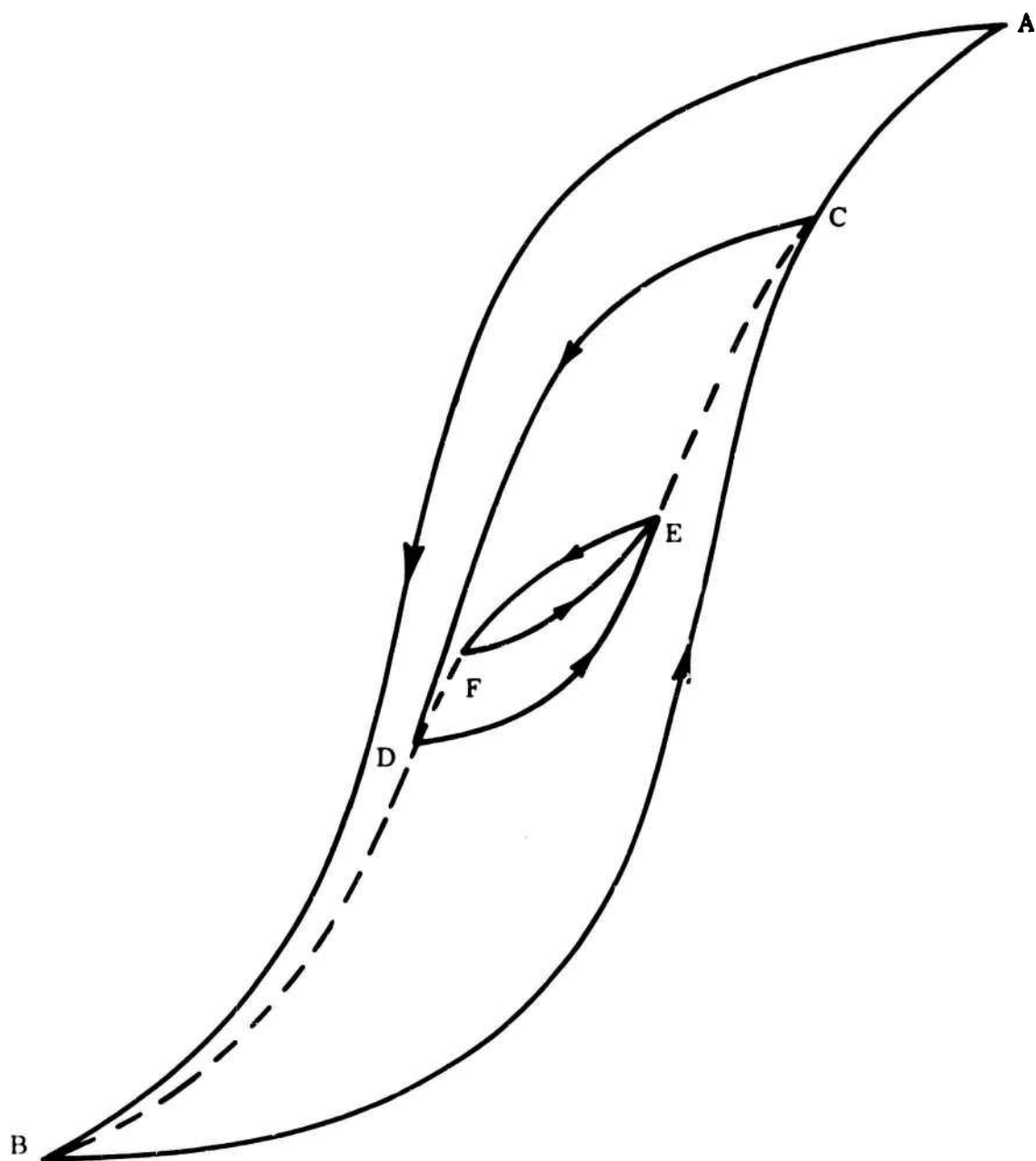
Figure 4-1. Typical BH Curves

The implementation of these basic rules is illustrated by the logic chart of Figure 4-2. The two disconnected portions of this chart are a result of the nature of the numerical integration subroutine used in the GOLD-N-ROD program. This subroutine achieves a balance between accuracy and economy by choosing the integration interval so that the estimated errors meet a set of specified error criteria. Only if the criteria are satisfied is the interval considered a good integration step. It is only at such a step that the logic based on the above rules is applied. However, the integration method requires the computation of derivatives, and therefore of torques, at every interval and at certain subintervals. At every interval or subinterval, the calculation of magnetic moments and torques is based on the value of the flux density at the most recent good step.

At the initial time, the BH point is assumed to be on the major hysteresis loop, as stated previously. In order to determine whether the point lies on the ascending or descending branch of this loop, the initial values of the instantaneous time derivatives of the earth's field components are computed. If the derivative in question has a positive value, the initial point lies on the ascending curve and the ascending-descending index (D-A index) is set equal to +1. Conversely, if the initial value of $\dot{H}$ is negative, the initial point is on the descending branch, and the D-A index is set equal to -1.

In order to use the reversal criterion (as explained later) at the next good integration step, an artificial increment in the field must be created, which corresponds to the time increment prior to the initial time. Only the algebraic sign of this artificial increment is used in the logic, and the numerical value is of no consequence.

Each BH curve is identified by the coordinates of its beginning point. The end point of the curve is the beginning point of the prior curve, in accordance with the rules previously explained. Because of the necessity of sometimes returning to a prior curve, the beginning point coordinates of every curve must be stored, unless they are intentionally erased at a later time. The section of the memory serving this function is called the curve array. The beginning point coordinates of each curve are identified by the curve array index (JHYS), which is assigned in chronological order. In accordance with this system, the branch of the major loop on which the initial point lies is assigned JHYS equal to 2, and the beginning point coordinates are stored in the curve array with this index value. The other branch of the major loop is assigned JHYS equal to 1, and its beginning point coordinates are stored accordingly. Henceforth, the beginning point of the curve presently used always has an index equal to JHYS, the highest value of the index. The end point of the present curve, being the beginning point of the prior curve, has an index equal to JHYS-1.

At the initial time, the flux density in the rods is computed from the magnetic field components (in the satellite body frame), using the analytical approximation for the major loop, which has been stored as one of the eleven reference curves.

At any interval, including the initial time, the magnetic moments of the rods are computed from their flux densities. After this has been done for both the Y and Z-axis rods,

A

Test NTEST(I) = 0

Not Exceeded

No Reversal of Ḣ, Sign of D-A Index Remains the Same. Test Field for Exceeding End Point.

Ex-ceeded

Curve Arr
JHYS(I), i
by 2. Set
Equal to O
JHYS(I).

≤ 1

Follow Procedure for Both Y and Z Axes. Set NTEST(I) = 0. Set New Previous Field Increment Equal to Old Present One. Compute Present Field Increment. Set New Previous Flux Density Equal to Old Present One.

·0

Compute Product of Last Two Field In-crements. Test Sign of Product.

< 0

Reversal of
Sign of D-A
Reversed an

0

Set Present Increment Equal to Negative of Previous One.

C
E

At Good Integration Steps Only → Enter HYSTOR from OUTPUT. NOPT = 2. → Test (T-T₀-.01)

> 0

= 0

Set JHYS(1) = JHYS(2) = 2. → Store Variables on Tape and Return to OUTPUT.

At Every Integration Step → Enter HYSTOR from DERIV. NOPT = 1 → Calculate Magnetic Field Components Test (T-T₀-.01)

·0

≤ 0

For Both Y and Z Axes, Compute Artificial Previous Field Increment, D-A Index, Beginning and End Point Coordinates, and Flux Density. Set up New Previous Field Value Equal to Present Field Value, for Next Interval. → Compute Magnetic Moments and Torques

ve Array Index,
'S(I), is Reduced
!. Set NTEST(J)
al to One. Test
'S(I).

> I

≤ I   Call
    Exit

Exceeded

Set $I_C = 11$

< 0

$I_C = 10$

sal of H has Occurred.
if D-A Index is
sed and Checked.

OK

Test Curve Array Index,
JHYS(I), to Determine
Whether Memory Capacity
Will be Exceeded.

JHYS(I) < 400

Curve Array Index, JHYS(I),
is Increased by One. Co-
ordinates of New Beginning
Point are Set Equal to Previous
Values of Field and Flux Density.
Set NTEST(I) = I.

Test Field for
Exceeding End
Point.

Test
NTEST(I)

= 1

Compute the Range, HHE(I).
Compute Flux Density Diff-
erence Between Beginning I
of Each Reference Curve an
That of New Present Curve.
Test the Difference, HGA(I(

Wrong

Call
Exit

JHYS(I) ≥ 400

Call
Exit

Not Exceeded

Return to DERIV

Test
NTEST(I)

= 0

Not
Exceeded

Reversal of H, Sign of
A Index Remains the
ne. Test Field for
ceeding End Point.

Ex-
ceeded

Curve Array Index,
JHYS(I), is Reduced
by 2. Set NTEST(I)
Equal to One. Test
JHYS(I).

> I

Exceeded

≤ 1

Call
Exit

-0

Compute Product of
Last Two Field In-
crements. Test
Sign of Product.

< 0

Reversal of H has Occurred.
Sign of D-A Index is
Reversed and Checked.

OK

Test Curve Array Index,
JHYS(I), to Determine
Whether Memory Capacity
Will be Exceeded.

JHYS(I) < 400

Curve Array Index, JHYS(I),
is Increased by One. Co-
ordinates of New Beginning
Point are Set Equal to Previous
Values of Field and Flux Density.
Set NTEST(I) = I.

Test Field for
Exceeding End
Point.

Test
NTEST(I)

Not Exceeded

0

et Present Increment
qual to Negative of
Previous One.

Wrong

Call
Exit

JHYS(I) ≥ 400

Call
Exit

e Variables on
and Return
UTPUT.

Compute Magnetic
Moments and Torques

Return to DERIV

Set $I_C = 11$

< 0

$I_C = 10$

Set ICUR(I) = I_C.
Compute Beginning
and End Values of
Interpolation
Coefficient.

Compute Flux Density.
Set up New Previous
Field Value Equal to
Present Value, for
Next Interval.

Store Variables on Tape
and Return to OUTPUT.

≥ 2

t

$T(1)$

$= 1$

Compute the Range, HHE(1).
Compute Flux Density Diff-
erence Between Beginning Point
of Each Reference Curve and
That of New Present Curve.
Test the Difference, HGA(IC).

≥ 0

Test I_C

≤ 1

Set ICUR(1) = 2. Inter-
polation Coefficient = 0.
Compute Flux Density.
Set up New Previous
Field Value Equal to
Present Field Value,
for Next Interval.

< 0

$1 \leq I_C \leq 9$

Figure 4-2. BH Curve Tracing Logic

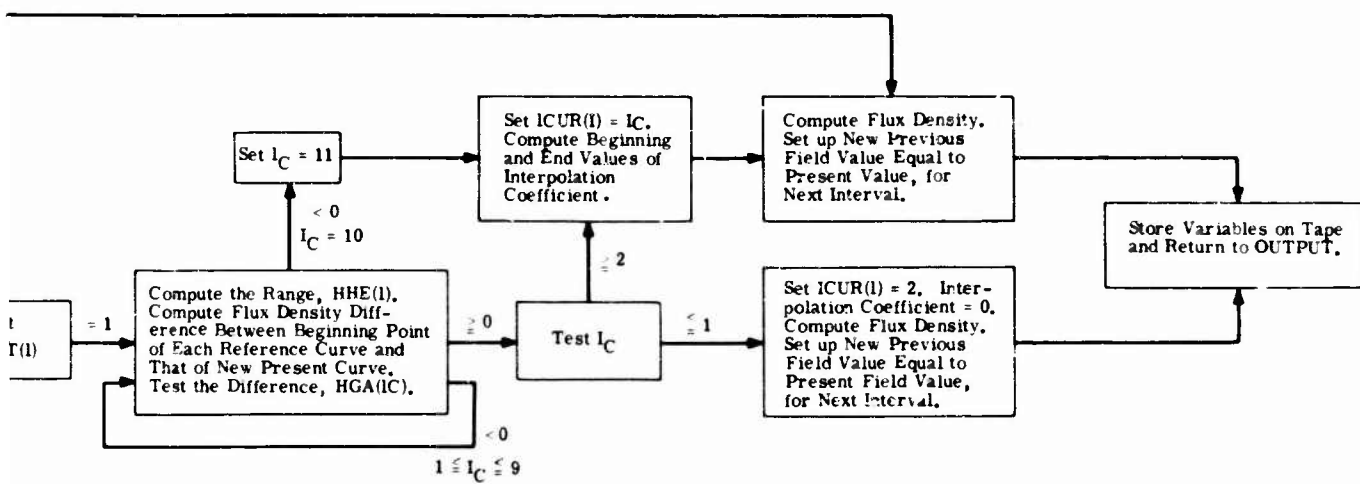the values are added to the respective components of the fixed or residual magnetic moment of the satellite to obtain the components of the total magnetic moment. (The fixed magnetic moments of the NWL satellite are negligible.) The components of the magnetic torque are then computed from those of the satellite magnetic moment and those of the earth's magnetic field.

At any good integration step, it is necessary to detect a reversal in the sign of the increment of the field, H. Such reversals occur at points C, D, E, and F, in Figure 4-1. Detection of reversals is accomplished by comparing the last two increments. If they are of like sign, as manifested by a positive product, no reversal has occurred. With no reversal, the D-A index remains the same as previously. If the last two increments in H are of unlike sign, as manifested by a negative product, a reversal has occurred. The sign of the D-A index is then reversed and checked. A reversal also has occurred if the last increment in H is zero, as manifested by a zero product. The procedure illustrated in the chart treats this case as though the product was negative. This prevents the occurrence of a zero product at the next interval, which would otherwise cause a second apparent reversal for a single occurrence of a zero increment. The logic shown in the chart will correctly determine the occurrence of reversals at the following time interval for any sign (or zero value) of the increment pertaining to that interval.

After any reversal, a new BH curve must be derived, and is then treated as the present curve. This is done by using the coordinates of the beginning and end points, as explained later. The beginning point coordinates are the values of B and H at the time interval prior to the one when the reversal was detected. These prior values have always been stored, to facilitate this, because it is never known when the next interval will produce a reversal. These beginning point coordinates are assigned the next available JHYS number and stored in the curve array. The coordinates of the end point of the new curve are the values then available in the curve array under the index JHYS-1.

Whether a reversal has occurred or not, the value of H must be tested to determine whether it is beyond the end point of the present BH curve. If not, and if no reversal has occurred, the flux density is computed by using the present curve. If a reversal has just occurred, but H is not beyond the end point of the new curve, that new curve is used in determining the flux density.

Whenever the value of H lies beyond the end point of the present curve, regardless of the occurrence of a reversal, the last two curves must be erased from the memory (curve array), and the curve prior to those two must be considered for use. Since it is possible that the value of H lies beyond the end point of any new curve, the test must be repeated, as shown in the chart, until a satisfactory end point has been determined. The end point is acceptable if the value of H does not lie beyond it. The coordinates of the acceptable end point, together with those of the beginning point of the corresponding curve, are used to derive a new BH curve (which then becomes the present curve) by a method explained later. The flux density is then computed from this new curve.

In the program, all B-H curves are considered as ascending curves. When the path of the BH point is along a descending curve, it is considered for computational purposes that the signs of B and H are reversed for the entire history of the rods. Then the descending curve becomes an ascending one. The computed value of the flux density is multiplied by the D-A index. The use of this index in appropriate places automatically inverts curves and multiplies computed values by -1 whenever necessary, in order to use the basic ascending curves and associated logic for both ascending and descending curves.

At every good integration step, the variables required for printout are stored on tape.

4.2.2 Inputs

The inputs for the hysteresis torque subroutine include two constants and 88 coefficients. One constant is the value of the external magnetic field corresponding to the tip of the major hysteresis loop. The second is a conversion factor to compute the magnetic moments from the flux densities. The 88 coefficients are those of eleven seventh-degree polynomials, which are used to represent the BH curves. These are discussed in detail in Section 4.3.1.

4.2.3 Equations

Certain of the computations are performed at every integration step and others only at good integration steps. This is accomplished by entering the HYSTOR subroutine from other subroutines. At every integration step, HYSTOR is entered from DERIV, with the entry point index, NOPT, equal to 1. The computations described in Section 4.2.3.1 are then performed. At good steps only, HYSTOR is entered from OUTPUT, with the entry point index equal to 2. The computations described in Section 4.2.3.2 are then performed.

4.2.3.1 Computations at Every Integration Step

At every integration step, certain of the following computations are performed. At every time interval, the components of the earth's magnetic field are computed, as described in Section 4.2.3.1a. At the initial time, T_o, the computations described in Section 4.2.3.1b are done. At every time interval, the magnetic moments and torques are computed, as described in Section 4.2.3.1c.

The time, T, is tested. If

$$T - T_o - 0.01 \leqq 0, \tag{1}$$

the time, T, is considered equal to the initial time, T_o. The small increment assures that the correct choice will be made, regardless of roundoff errors.

a. Components of the Earth's Magnetic Field - The components of the earth's
    magnetic field, in spherical coordinates, B_R, B_θ, and B_ϕ, are computed in
    a subroutine adapted from the program used by the Armed Forces Special
    Weapons Command at Kirtland Air Force Base, New Mexico. This subroutine
    requires the altitude, A_{LT}, latitude, λ, and longitude, Ω_V, of the satellite,
    as inputs. These are all available from previous subroutines. The components
    in spherical coordinates are converted to those in the orbital and satellite
    reference frames. Use is made of the right ascension of the satellite, Ω_T,
    and the right ascension of the ascending node, Ω_N, also available from previous
    subroutines. These celestial angles are measured from a baseline along the
    vernal equinox. The positive direction of this baseline, corresponding to zero
    values of the angles, is from the heliocenter to the geocenter at the time of
    vernal equinox. This is opposite from the customary reference direction.

    The difference in the longitudes of the satellite and of the ascending node is

    $$\Omega_M = \Omega_T - \Omega_N. \tag{2}$$

    The $[D]$ matrix is used to convert from the spherical coordinate frame to
    the orbital frame, RPQ. The elements of the $[D]$ matrix are

    $$D_{11} = 1, \tag{3}$$

    $$D_{22} = \sin \nu \, \cos \Omega_M, \tag{4}$$

    $$D_{23} = -\frac{\cos \nu}{\cos \lambda}, \tag{5}$$

    $$D_{32} = -D_{23}, \tag{6}$$

    $$D_{33} = D_{22}, \tag{7}$$

    $$D_{12} = D_{13} = D_{21} = D_{31} = 0, \tag{8}$$

    where ν is the orbital inclination angle.

    The components of the earth's magnetic field, in the orbital frame, are

    $$\begin{bmatrix} H_R \\ H_P \\ H_Q \end{bmatrix} = [D] \begin{bmatrix} -B_R \\ B_\theta \\ B_\phi \end{bmatrix} \tag{9}$$

    The $[E]$ matrix is used to convert from the orbital frame to the satellite frame.
    The elements of this matrix are computed in a previous subroutine. The com-
    ponents of the field, in the satellite frame, are

$$
\begin{bmatrix} H_{13} \\ H_{11} \\ H_{12} \end{bmatrix} = [E] \begin{bmatrix} H_R \\ H_P \\ H_Q \end{bmatrix} . \tag{10}
$$

H_{13} is the X_1 component, H_{11} is the Y_1 component, and H_{12} is the Z_1 component.

b. <u>Computations at the Initial Time, T_O</u> - The logic requires the time increment in the magnetic field. At the initial time, T_O, the field increment would correspond to the time interval prior to T_O. This increment is not available, and therefore it must be generated artificially. Only the algebraic sign of the increment has any effect, not the numerical value.

The increments due to satellite attitude motion, satellite orbital motion, and earth spin motion are computed and combined. The increments due to attitude motion depend on the time derivatives of the $[E]$ matrix elements. These are designated by the additional subscript, D:

$$
E_{D21} = E_{31}\,\omega_{X1} - E_{11}\,\omega_{Z1} + E_{22}\,\dot{\eta} , \tag{11}
$$

$$
E_{D22} = E_{32}\,\omega_{X1} - E_{12}\,\omega_{Z1} - E_{21}\,\dot{\eta} , \tag{12}
$$

$$
E_{D23} = E_{33}\,\omega_{X1} - E_{13}\,\omega_{Z1} , \tag{13}
$$

$$
E_{D31} = E_{11}\,\omega_{Y1} - E_{21}\,\omega_{X1} + E_{32}\,\dot{\eta} , \tag{14}
$$

$$
E_{D32} = E_{12}\,\omega_{Y1} - E_{22}\,\omega_{X1} - E_{31}\,\dot{\eta} , \tag{15}
$$

$$
E_{D33} = E_{13}\,\omega_{Y1} - E_{23}\,\omega_{X1} , \tag{16}
$$

where η is the orbital angular velocity, and the body axis rates are ω_{X1}, ω_{Y1}, and ω_{Z1}.

The required time derivatives of the components of the earth's magnetic field are

$$
H_{1D1} = E_{D21} H_R + E_{D22} H_P + E_{D23} H_Q , \tag{17}
$$

$$
H_{1D2} = E_{D31} H_R + E_{D32} H_P + E_{D33} H_Q , \tag{18}
$$

or

$$
H_{1DI} = E_{D, I+1, 1} H_R + E_{D, I+1, 2} H_P + E_{D, I+1, 3} H_Q . \tag{19}
$$

The subscript I is 1 for the Y axis and 2 for the Z axis. The same set of equations is used for both axes, in most cases. Only one set of equations, with subscript I, will be included hereafter.

4-14

The increments in the field due to the satellite orbital motion and earth spin motion depend upon extrapolated values of the satellite's latitude and longitude prior to T_o. The T_o value of the altitude is used, because the change would be so small, anyway.

The orbital angle prior to time zero is

$$\eta_D = \eta - \Delta \eta, \tag{20}$$

where $\Delta \eta$ is the initial integration interval. The extrapolated prior latitude is

$$\lambda_D = \sin^{-1} (\sin \nu \, \sin \eta_D). \tag{21}$$

The corresponding longitude is computed from various angles. The sidereal angle of Greenwich is

$$\Omega_{GD} = \Omega_G - \dot{\Omega}_G \frac{\Delta \eta}{\dot{\eta}}, \tag{22}$$

where Ω_G is the value at T_o, $\dot{\Omega}_G$ is the earth's spin rate, and $\dot{\eta}$ is the satellite's orbital angular velocity.

The right ascension of the ascending node is

$$\Omega_{ND} = \Omega_N - \dot{\Omega}_N \frac{\Delta \eta}{\dot{\eta}}, \tag{23}$$

where Ω_N is the value at T_o and $\dot{\Omega}_N$ is the precession rate of the nodes. The right ascension of the satellite, Ω_{TD}, is found from

$$\sin \Omega_{TD} = \frac{\sin \Omega_{ND} \cos \eta_D + \cos \nu \cos \Omega_{ND} \sin \eta_D}{\cos \lambda_D}, \tag{24}$$

$$\cos \Omega_{TD} = \frac{\cos \Omega_{ND} \cos \eta_D - \cos \nu \sin \Omega_{ND} \sin \eta_D}{\cos \lambda_D}. \tag{25}$$

The extrapolated prior longitude is

$$\Omega_{VD} = \Omega_{TD} - \Omega_{GD}. \tag{26}$$

The corresponding difference in the longitudes of the satellite and of the ascending node is

$$\Omega_{MD} = \Omega_{TD} - \Omega_{ND}. \tag{27}$$

These values are used in the earth's magnetic field subroutine to find the extrapolated prior values of the field in spherical coordinates. The elements of the $[D]$ matrix are found from Equations (3) through (8), with Ω_{MD} used in place of Ω_M, and λ_D used in place of λ. Equations (9) and (10) are then used to compute D_{EH13}, D_{EH11}, and D_{EH12}, the components of the extrapolated prior field in the satellite reference frame. The artificial increments, due to orbital travel and earth's spin, are

$$D_{H11} = H_{11} - D_{EH11}, \tag{28}$$

$$D_{H12} = H_{12} - D_{EH12}. \tag{29}$$

The total artificial increments are

$$H_{HNI} = H_{1DI} \frac{\overset{\wedge}{\eta}}{\overset{\cdot}{\eta}} + D_{H1I} \tag{30}$$

The D-A index, H_{DAI} is determined in accordance with the algebraic sign of H_{HNI}

If $H_{HNI} < 0$, $H_{DAI} = -1$. \hfill (31)

If $H_{HNI} \geqq 0$, $H_{DAI} = +1$. \hfill (32)

The end point coordinates of the branch of the major hysteresis loop are

$$H_{HC1I} = H_{DAI} H_{FAH}, \tag{33}$$

$$H_{BC1I} = -H_{DAI} H_{FA1I}, \tag{34}$$

where H_{FAH} and $-H_{FA1I}$ are the coordinates of the positive tip of the loop.

The corresponding beginning point coordinates are

$$H_{HC2I} = -H_{HC1I}, \tag{35}$$

$$H_{BC2I} = -H_{BC1I}. \tag{36}$$

The argument of the polynomial used to find the flux density is the D-A-indexed difference between the field value and the beginning point value,

$$X = H_{DAI} (H_{1I} - H_{HC2I}). \tag{37}$$

The value, H_F, of the polynomial is computed. The flux density is

$$H_{BLI} = H_{DAI} H_F. \tag{38}$$

The increments in the field due to the satellite orbital motion and earth spin motion depend upon extrapolated values of the satellite's latitude and longitude prior to T_0. The T_0 value of the altitude is used, because the change would be so small, anyway.

The orbital angle prior to time zero is

$$\eta_D = \eta - \Delta \eta , \tag{20}$$

where $\Delta \eta$ is the initial integration interval. The extrapolated prior latitude is

$$\lambda_D = \sin^{-1} (\sin \nu \, \sin \eta_D). \tag{21}$$

The corresponding longitude is computed from various angles. The sidereal angle of Greenwich is

$$\Omega_{GD} = \Omega_G - \dot{\Omega}_G \frac{\Delta \eta}{\dot{\eta}} , \tag{22}$$

where Ω_G is the value at T_0, $\dot{\Omega}_G$ is the earth's spin rate, and $\dot{\eta}$ is the satellite's orbital angular velocity.

The right ascension of the ascending node is

$$\Omega_{ND} = \Omega_N - \dot{\Omega}_N \frac{\Delta \eta}{\dot{\eta}} , \tag{23}$$

where Ω_N is the value at T_0 and $\dot{\Omega}_N$ is the precession rate of the nodes. The right ascension of the satellite, Ω_{TD}, is found from

$$\sin \Omega_{TD} = \frac{\sin \Omega_{ND} \cos \eta_D + \cos \nu \, \cos \Omega_{ND} \sin \eta_D}{\cos \lambda_D} , \tag{24}$$

$$\cos \Omega_{TD} = \frac{\cos \Omega_{ND} \cos \eta_D - \cos \nu \, \sin \Omega_{ND} \sin \eta_D}{\cos \lambda_D} . \tag{25}$$

The extrapolated prior longitude is

$$\Omega_{VD} = \Omega_{TD} - \Omega_{GD} . \tag{26}$$

The corresponding difference in the longitudes of the satellite and of the ascending node is

$$\Omega_{MD} = \Omega_{TD} - \Omega_{ND} . \tag{27}$$

These values are used in the earth's magnetic field subroutine to find the extrapolated prior values of the field in spherical coordinates. The elements of the $[D]$ matrix are found from Equations (3) through (8), with Ω_{MD} used in place of Ω_M, and λ_D used in place of λ. Equations (9) and (10) are then used to compute D_{EH13}, D_{EH11}, and D_{EH12} the components of the extrapolated prior field in the satellite reference frame. The artificial increments, due to orbital travel and earth's spin, are

$$D_{H11} = H_{11} - D_{EH11}, \tag{28}$$

$$D_{H12} = H_{12} - D_{EH12}. \tag{29}$$

The total artificial increments are

$$H_{HNI} = H_{1DI} \frac{\hat{\eta}}{\dot{\eta}} + D_{H1I} \tag{30}$$

The D-A index, H_{DAI} is determined in accordance with the algebraic sign of H_{HNI}

If $H_{HNI} < 0$, $H_{DAI} = -1$. \hfill (31)

If $H_{HNI} \geq 0$, $H_{DAI} = +1$. \hfill (32)

The end point coordinates of the branch of the major hysteresis loop are

$$H_{HC1I} = H_{DAI} H_{FAH}, \tag{33}$$

$$H_{BC1I} = -H_{DAI} H_{FA11}, \tag{34}$$

where H_{FAH} and $-H_{FA11}$ are the coordinates of the positive tip of the loop.

The corresponding beginning point coordinates are

$$H_{HC2I} = -H_{HC1I}, \tag{35}$$

$$H_{BC2I} = -H_{BC1I}. \tag{36}$$

The argument of the polynomial used to find the flux density is the D-A-indexed difference between the field value and the beginning point value,

$$X = H_{DAI} (H_{1I} - H_{HC2I}). \tag{37}$$

The value, H_F, of the polynomial is computed. The flux density is

$$H_{BLI} = H_{DAI} H_F. \tag{38}$$

The increments in the field due to the satellite orbital motion and earth spin motion depend upon extrapolated values of the satellite's latitude and longitude prior to T_o. The T_o value of the altitude is used, because the change would be so small, anyway.

The orbital angle prior to time zero is

$$\dot{\eta}_D = \eta - \Delta \eta , \tag{20}$$

where $\Delta \eta$ is the initial integration interval. The extrapolated prior latitude is

$$\lambda_D = \sin^{-1} (\sin \nu \, \sin \eta_D). \tag{21}$$

The corresponding longitude is computed from various angles. The sidereal angle of Greenwich is

$$\Omega_{GD} = \Omega_G - \dot{\Omega}_G \, \frac{\Delta \eta}{\dot{\eta}} , \tag{22}$$

where Ω_G is the value at T_o, $\dot{\Omega}_G$ is the earth's spin rate, and $\dot{\eta}$ is the satellite's orbital angular velocity.

The right ascension of the ascending node is

$$\Omega_{ND} = \Omega_N - \dot{\Omega}_N \, \frac{\Delta \eta}{\dot{\eta}} , \tag{23}$$

where Ω_N is the value at T_o and $\dot{\Omega}_N$ is the precession rate of the nodes. The right ascension of the satellite, Ω_{TD}, is found from

$$\sin \Omega_{TD} = \frac{\sin \Omega_{ND} \cos \eta_D + \cos \nu \cos \Omega_{ND} \sin \eta_D}{\cos \lambda_D} , \tag{24}$$

$$\cos \Omega_{TD} = \frac{\cos \Omega_{ND} \cos \eta_D - \cos \nu \sin \Omega_{ND} \sin \eta_D}{\cos \lambda_D} . \tag{25}$$

The extrapolated prior longitude is

$$\Omega_{VD} = \Omega_{TD} - \Omega_{GD} . \tag{26}$$

The corresponding difference in the longitudes of the satellite and of the ascending node is

$$\Omega_{MD} = \Omega_{TD} - \Omega_{ND} . \tag{27}$$

These values are used in the earth's magnetic field subroutine to find the extrapolated prior values of the field in spherical coordinates. The elements of the $[D]$ matrix are found from Equations (3) through (8), with Ω_{MD} used in place of Ω_M, and λ_D used in place of λ. Equations (9) and (10) are then used to compute D_{EH13}, D_{EH11}, and D_{EH12}, the components of the extrapolated prior field in the satellite reference frame. The artificial increments, due to orbital travel and earth's spin, are

$$D_{H11} = H_{11} - D_{EH11}, \tag{28}$$

$$D_{H12} = H_{12} - D_{EH12}. \tag{29}$$

The total artificial increments are

$$H_{HNI} = H_{1DI} \frac{\dot{\eta}}{\eta} + D_{H1I} \tag{30}$$

The D-A index, H_{DAI} is determined in accordance with the algebraic sign of H_{HNI}

If $H_{HNI} < 0$, $H_{DAI} = -1.$ \hfill (31)

If $H_{HNI} \geq 0$, $H_{DAI} = +1.$ \hfill (32)

The end point coordinates of the branch of the major hysteresis loop are

$$H_{HC1I} = H_{DAI} H_{FAH}, \tag{33}$$

$$H_{BC1I} = -H_{DAI} H_{FA1l}, \tag{34}$$

where H_{FAH} and $-H_{FA1l}$ are the coordinates of the positive tip of the loop.

The corresponding beginning point coordinates are

$$H_{HC2I} = -H_{HC1I}, \tag{35}$$

$$H_{BC2I} = -H_{BC1I}. \tag{36}$$

The argument of the polynomial used to find the flux density is the D-A-indexed difference between the field value and the beginning point value,

$$X = H_{DAI} (H_{1I} - H_{HC2I}). \tag{37}$$

The value, H_F, of the polynomial is computed. The flux density is

$$H_{BLI} = H_{DAI} H_F. \tag{38}$$

The value, H_{1I}, of the magnetic field component is assigned to H_{HMI}, the symbol for the prior value so that it will be available as such at the next time interval.

$$H_{HMI} = H_{1I}. \tag{39}$$

c. <u>Magnetic Moments and Torques</u> - The magnetic moments and torques are computed at every time interval. The magnetic moments are computed from

$$H_{DBY} = H_{DC} H_{BL1} + H_{CY}, \tag{40}$$

$$H_{DBZ} = H_{DC} H_{BL2} + H_{CZ}. \tag{41}$$

where H_{DC} is the constant for converting from flux density at the center of one rod to total magnetic moment of a set of two parallel rods. For the NWL satellite, this factor is 80.067×10^{-6} foot-pounds per oersted-gauss. H_{CX}, H_{CY}, and H_{CZ} are the components of the fixed or residual magnetic moment of the satellite. For the NWL satellite, this magnetic moment is negligible.

The components of the magnetic hysteresis torque are

$$T_{MHX} = H_{DBY} H_{12} - H_{DBZ} H_{11}, \tag{42}$$

$$T_{MHY} = H_{DBZ} H_{13} - H_{CX} H_{12}, \tag{43}$$

$$T_{MHZ} = H_{CX} H_{11} - H_{DBY} H_{13}. \tag{44}$$

These torques are added to the other torques acting on the satellite.

The program then returns to the DERIV subroutine.

4.2.3.2 Computations at Good Integration Steps

At good integration steps only, the logic (which implements the basic rules for tracing hysteresis loops) is employed.

The time, T, is tested by inequality (1). If this inequality holds, T is considered equal to T_o, and the curve array indexes for both axes are set equal to 2,

$$J_{HYS1} = 2, \tag{45}$$

$$J_{HYS2} = 2. \tag{46}$$

The program then returns to the output subroutine, and the required variables are stored on tape for later printout.

If
$$T - T_o - 0.01 > 0,$$

(47)

the time is later than the initial time, and the ensuing logic is employed for both axes by the index I taking the values 1 and 2.

The index N_{TESTI} is set equal to zero for possible later use.

The new value of the previous field increment is set equal to the old value of the present increment

$$H_{HPI} = H_{HNI}.$$

(48)

The new value of the present increment is computed from the appropriate values of the field.

$$H_{HNI} = H_{1I} - H_{HMI}.$$

(49)

Writing the new values over the old ones automatically erases the latter from the memory.

In a similar manner, the new value of the previous flux density is set equal to the old present value,

$$H_{BMI} = H_{BLI}.$$

(50)

The product of the present and previous field increments is computed,

$$H_{HQI} = H_{HNI} H_{HPI}.$$

(51)

If this product is positive, no reversal in $\dot{H}$ has occurred, and the procedure of Section b below is followed.

If the product is negative, a reversal in $\dot{H}$ has occurred, and the procedure of Section a below is followed.

If the product is zero, a reversal in $\dot{H}$ has occurred. In this case the present increment is set equal to the negative of the previous increment,

$$H_{HNI} = -H_{HPI}.$$

(52)

and the procedure of Section a below is followed.

a. Procedure With a Reversal of $\dot{H}$ - When a reversal of $\dot{H}$ occurs, the sign of the D-A index is reversed,

$$H_{DAI} = -H_{DAI}.$$

(53)

The new value of the index is checked for agreement with the sign of the present field increment. If

$$H_{DAI} H_{HNI} < 0,$$

(54)

4-18

the program is stopped. If

$$H_{DAI} H_{HNI} \gtreqless 0, \tag{55}$$

the procedure continues.

The curve array index is checked next. If

$$J_{HYSI} - 400 \gtreqless 0, \tag{56}$$

the remaining storage is insufficient, and the program is stopped. If

$$J_{HYSI} - 400 < 0, \tag{57}$$

sufficient storage remains, and the program continues.

The curve array index is increased by one,

$$J = J_{HYSI} + 1, \tag{58}$$

$$J_{HYSI} = J. \tag{59}$$

The new beginning point coordinates are set equal to the previous values of the field and flux density.

$$H_{HCJI} = H_{HMI}, \tag{60}$$

$$H_{BCJI} = H_{BMI}, \tag{61}$$

These coordinates are automatically stored in the curve array.

The index N_{TESTI} is set equal to 1, as an indication that a new BH curve must be used.

The value of the field is tested to determine whether it exceeds the new end point. To facilitate this, a temporary index is needed,

$$J = J_{HYSI}. \tag{62}$$

The H-coordinate of the new end point is then $H_{HC, J-1, I}$. The D-A-indexed difference between the field and this coordinate is

$$T_{EMPI} = H_{DAI} (H_{1I} - H_{HC, J-1, I}). \tag{63}$$

If

$$T_{EMPI} \gtreqless 0, \tag{64}$$

the field exceeds the new end point. The curve array index is then reduced by two,

$$J_{HYSI} = J_{HYSI} - 2. \tag{65}$$

The index N_{TESTI} is again set equal to 1. Since J_{HYSI} was reduced, it is advisable to check that its value is not too low. The minimum allowable value is two. If

$$J_{HYSI} - 1 = 0, \tag{66}$$

the index is one or less, and the program is stopped. If

$$J_{HYSI} - 1 > 0, \tag{67}$$

the index is at least two, and the program continues.

The reduction in the index results in the admission of a new BH curve, with new beginning and end points. The test of the field for exceeding the new end point is repeated by again using Equations (62) and (63). As long as inequality (64) holds, the repetition is continued. Eventually, when

$$T_{EMPI} < 0, \tag{68}$$

a curve has been identified whose end point is not exceeded by the field. The index N_{TESTI} is then tested and found to be positive. The range of the new BH curve is computed,

$$H_{HEI} = H_{DAI} (H_{HC, J-1, I} - H_{HCJI}). \tag{69}$$

Two of the eleven stored polynomials are selected for interpolation. This is accomplished by taking the difference, H_{GAIC}, between the beginning value, $H_{FA, IC, 1}$ of each of the stored polynomials and the D-A-indexed value of the flux density, H_{BCJI}, corresponding to the beginning point of the new BH curve which is to be interpolated.

$$H_{GAIC} = H_{FA, IC, 1} - H_{DAI} H_{BCJI}. \tag{70}$$

The index I_C runs from one to ten.

If H_{GAIC} is found to be positive with I_C equal to one, it means that the beginning point lies outside the end of the major loop. (This may be due to roundoff error, or a poor choice of the major loop in the first place.) In this case, I_C is verified as being one, and the major loop is used for computing the flux density. The argument of the polynomial is the D-A-indexed difference between the field and the beginning point coordinate,

$$H_{HDI} = H_{DAI} (H_{1I} - H_{HCJI}).$$ (71)

The index I_{CURI} is set equal to two, indicating that the upper interpolation curve is the one above the major loop, and the lower one is the major loop. The interpolation coefficient is set equal to zero, so that, in effect, the major loop is used. The value of the polynomial is H_F, and the flux density is found from Equation (38). The new value of the previous field for the next time increment is set equal to the old present value by using Equation (39).

If H_{GAIC} is found to be positive for a certain value of I_C between two and ten, inclusive, the stored curve corresponding to this value is the upper interpolation curve. The curve corresponding to $I_C - 1$ is the lower interpolation curve.

If the difference given by Equation (70) is found to be negative with I_C equal to ten, the index I_C is set equal to eleven.

After I_C has been determined to be between two and eleven, inclusive, the beginning point value of the interpolation coefficient is found as the ratio of the appropriate differences in flux density coordinates,

$$H_{KAI} = \frac{-H_{GA, IC-1}}{H_{GAIC} - H_{GA, IC-1}} .$$ (72)

The value of the flux density, H_{ILI}, from the lower interpolation curve, $I_C - 1$, is found from its polynomial, using the range found from Equation (69) as the argument. Similarly, the value, H_{IUI}, from the upper interpolation curve, I_C, is found.

The end point value of the interpolation coefficient is found as the ratio of the appropriate flux density differences,

$$H_{KCI} = \frac{H_{DAI} H_{BC, J-1, I} - H_{ILI}}{H_{IUI} - H_{ILI}} .$$ (73)

The index

$$I_{CURI} = I_C.$$ (74)

is used henceforth to indicate the upper interpolation curve.

The argument of the polynomial is computed from Equation (71). This is used in the polynomials representing the interpolation curves. The value from the lower interpolation curve is designated H_{FLI}, and that from the upper one is H_{FUI}.

The parabolically sliding interpolation coefficient is

$$H_{KLI} = H_{KAI} + (H_{KCI} - H_{KAI}) \left(\frac{H_{HDI}}{H_{HEI}}\right)^2 .$$

(75)

The flux density is computed by interpolation between the interpolation curves,

$$H_{BLI} = H_{DAI} \left[H_{KLI} H_{FUI} + (1-H_{KLI}) H_{FLI} \right] .$$

(76)

The new value of the previous field for the next time interval is set up by using Equation (39).

The program then returns to the output subroutine, and the required variables are stored on tape for later printout.

b. <u>Procedure With No Reversal of $\dot{H}$</u> - With no reversal of $\dot{H}$, the D-A index remains unchanged. Nevertheless, the value of the field must be tested to determine whether it exceeds the end point of the present BH curve. This is done by means of Equations (62) and (63). The same procedure is followed as in the previous section. When inequality (68) is satisfied, a curve with a satisfactory end point has been found. If, during this procedure, inequality (64) was found to hold one or more times the index N_{TESTI} will have been set equal to one. Under this condition, the procedure of the last section will be followed, from Equation (69) onward.

If inequality (68) was satisfied the first time that T_{EMPI} was tested, the value of H did not exceed the end point of the present BH curve, so no new curve need be derived. The index N_{TESI} is tested and found equal to zero. Then the procedure of the last section will be followed, using Equation (71) to find the argument of the polynomial, the interpolation curves to find H_{FLI} and H_{FUI}, and continuing with Equations (75), (76), and (39).

4.3 CURVE-FITTING AND INTERPOLATION TECHNIQUES

The fitting of analytical expressions to the actual BH curves for the material, and the generation of an interpolation scheme, proved to be more difficult than the generation of the logical scheme. This difficulty was due to the shape of the BH curves, to the limited storage in the core memory of the computer, and to the necessity of obtaining economical running speeds. The last two factors required that the logic be simplified as much as possible, that a BH curve be derived from the least possible amount of information, and that the minimum amount of information about previous BH curves should be stored.

With all of these factors, as well as accuracy of the fit, taken into account, the final choice for the analytical function was a seventh degree polynomial. The manner of derivation of the coefficients, the interpolation scheme used in the digital computer

program, and related matters, are discussed in Section 4.3.1 below. Other methods which evidently have merit are discussed in Section 4.3.2. The methods which were investigated, but found unsatisfactory, are described in Section 4.3.3. These are included for the purpose of documentation and to prevent future effort from being expended along these lines without a realization of the shortcomings already found.

4.3.1 Seventh Degree Polynomials

BH curves for the rod material were obtained from the Allegheny Ludlum Steel Corporation, and processed as described in Section 4.3.1.1 below. The fitting of the polynomials and the interpolation of additional reference curves are described in Section 4.3.1.2. The interpolation scheme used in the digital program is described in Section 4.3.1.3.

4.3.1.1 Allegheny Ludlum Curves

Several sets of curves were obtained from the Allegheny Ludlum Steel Corporation. The set which was used is reproduced as Figure 4-3. The curves were taken for a ring sample of the material, and so they must be corrected for the demagnetization effect when applied to rods. For the rod dimensions used, the demagnetization factor, D_M, is 1.5×10^{-5} oersteds per gauss. The correction is applied to the field,

$$H_e = H_i + D_M B,\tag{1}$$

where B is the flux density at the center of the rod, H_i is the internal field at the center of the rod, and H_e is the applied field, which is external to the rod. H_i is then the value of the field which is plotted as the abscissa of the original set of curves in Figure 4-3. For the present purpose, H_e is the component along the rod axis of the earth's magnetic field at the satellite location. H_e is the abscissa of the derived set of curves in Figure 4-4. The derived set was obtained by replotting with a new abscissa value, in accordance with Equation (1). The values of H_e were actually obtained from the first part of a digital computer program which is described in Appendix II.

4.3.1.2 Curve-Fitting

The analytical expression used for fitting the BH curves is a seventh-degree polynomial. The coefficients were derived by means of the least squares method. The digital computer program used is described in detail in Appendix II.

The argument of the polynomial is the translated value of the field, that is the difference between the value of H_e at any point and the value at the beginning point of the curve being fitted. Likewise, the ordinates were translated by subtracting the beginning point value from each of the actual values. For the translated curve, the beginning point then has the coordinates (0, 0). The polynomial was forced to pass through this point by omitting the constant term from the general expression. To obtain the reference curves used in the digital program, the flux density was retranslated by adding the beginning point value, which thus becomes the constant in the polynomial. The argument of the polynomial, however, remains the translated value of the field. This is most useful in the main digital program, particularly for interpolation, as will be apparent later.
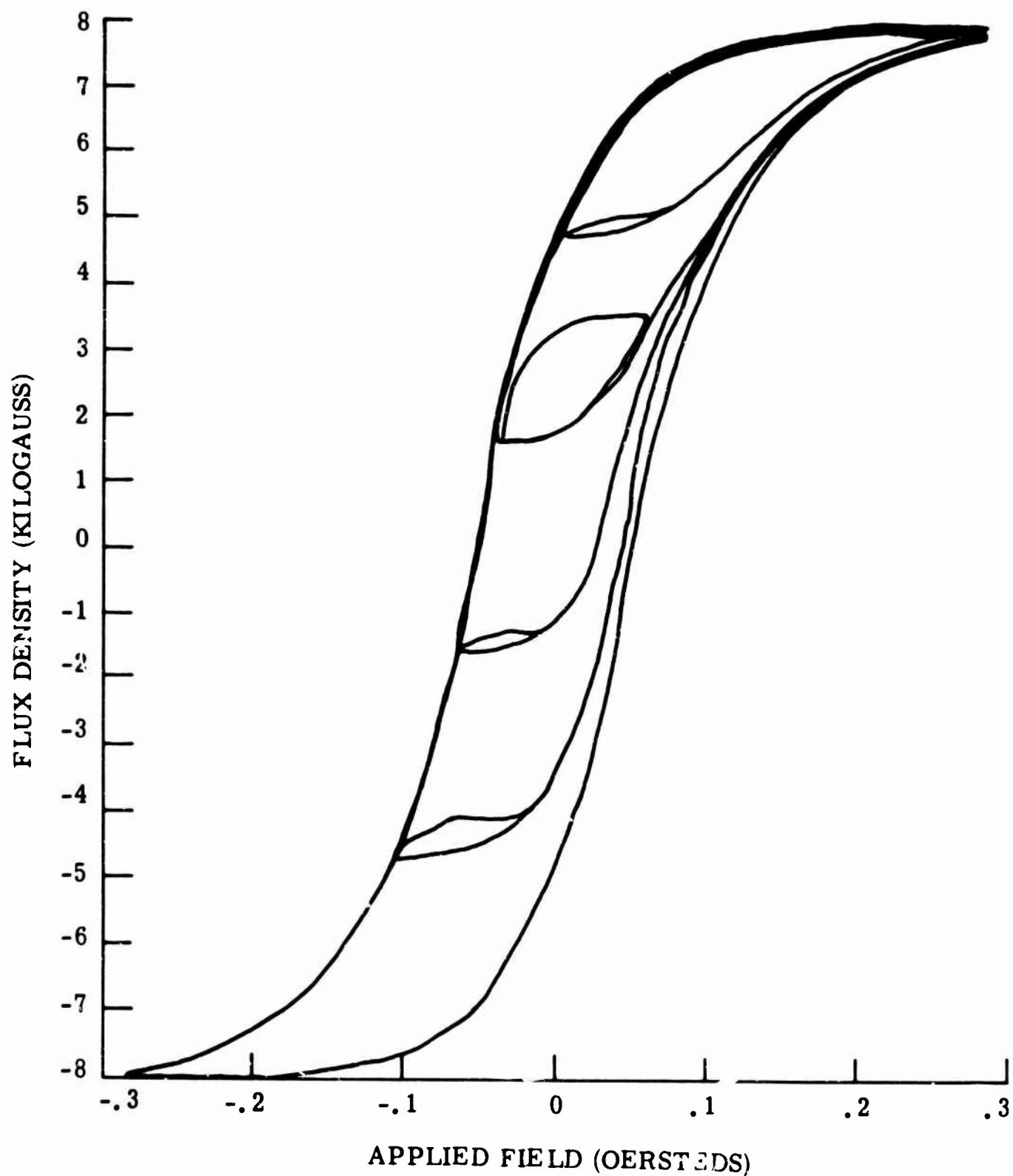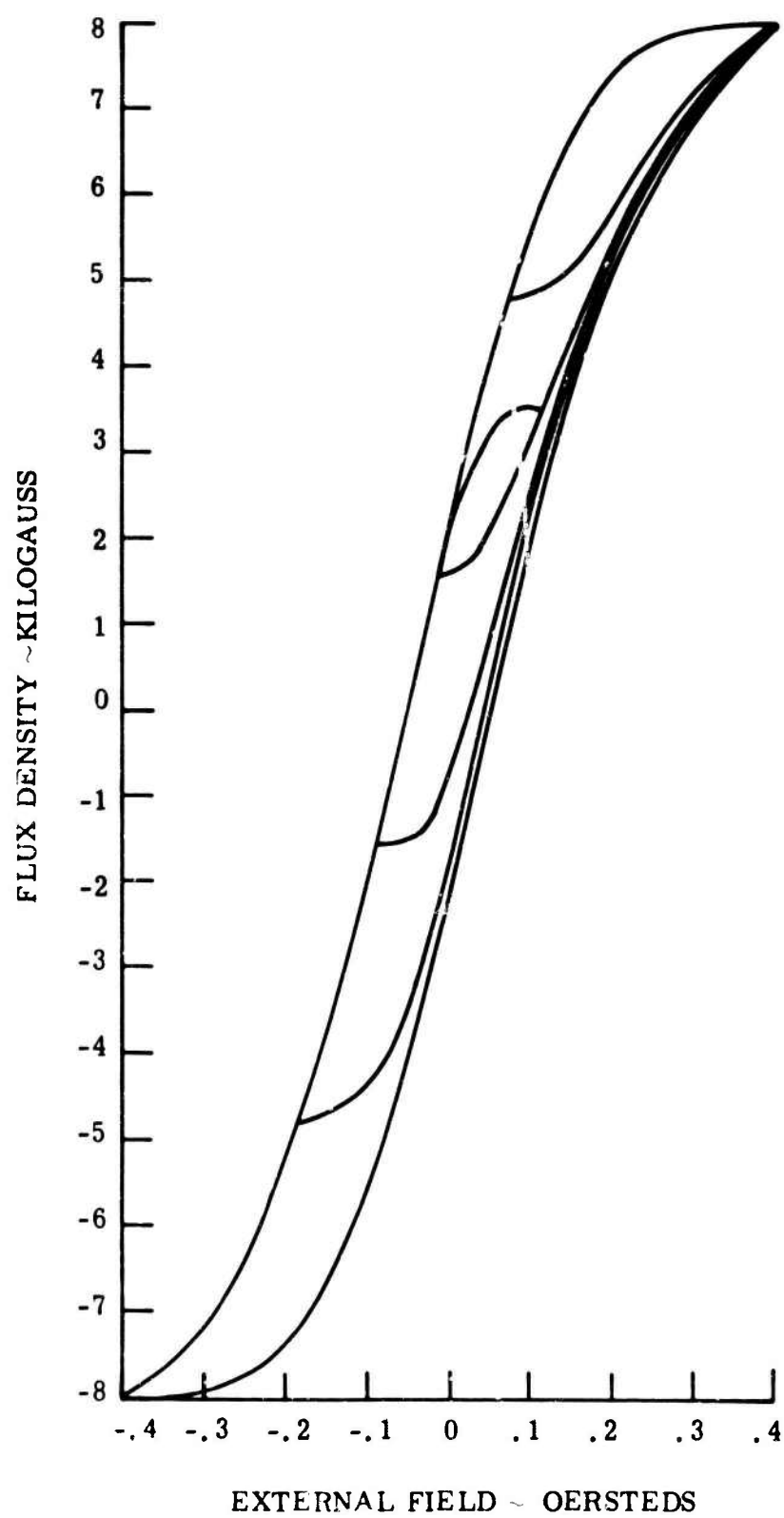
Figure 4-3. Original Allegheny-Ludlum 8-Kilogauss Data

Figure 4-4. Original Allegheny-Ludlum Data Modified for External Field

This procedure was applied to the ascending branch of the major hysteresis loop and to the four second-class curves of Figure 4-3. The second-class curves are the ascending ones which begin at various points along the descending branch of the major loop. The polynomials thus derived are plotted in Figure 4-5, and designated as curves number 1, 3, 5, 7, and 9. These designations correspond to the reference curve numbers used in the main program. Reference curve 11 is simply a horizontal line, and is used only when necessary to interpolate a curve above the uppermost BH reference curve available. (Attempts to use the descending branch of the major loop for this purpose yielded unsatisfactory results.)

Reference curves 2, 4, 6, 8, and 10, also shown in Figure 4-5, were obtained by interpolating between the odd-numbered curves.

The interpolation scheme described in the next section requires extrapolating each of the curves numbered 2 through 10 to reach the abscissa of the end point of the unextrapolated curve immediately below. These extrapolated sections are shown dashed in Figure 4-5. Each polynomial was fitted over the complete range, including the extrapolated portion.

The polynomials are of the form

$$B = \sum_{j=1}^{8} A_j H^{j-1} , \qquad (2)$$

where H is the translated field.

It became apparent in the course of the analysis that the maximum value of the earth's magnetic field at the perigee altitude would be about 0.55 oersteds. This value is greater than the 0.405 oersteds corresponding to the tip of the major loop in Figure 4-4. To overcome this deficiency, additional curves were requested from Allegheny Ludlum. These have not yet been received. Therefore, the curves of Figures 4-4 and 4-5 were adapted to the requirements of the program. This was accomplished by applying different stretching factors to the field and flux density scales. The factors used were derived by extrapolating the magnetization curve. This curve was assumed to go through the tips of the major loops of the 2, 4, 6, and 8 kilogauss sets of Allegheny Ludlum curves. The coordinates of these points are tabulated in Table 4-1.

TABLE 4-1. POINTS ON MAGNETIZATION CURVE

External Field, H_e (Oersteds)	Flux Density, B (Kilogauss)
0.084	2.0
0.140	4.0
0.202	6.0
0.405	8.0

A parabola,

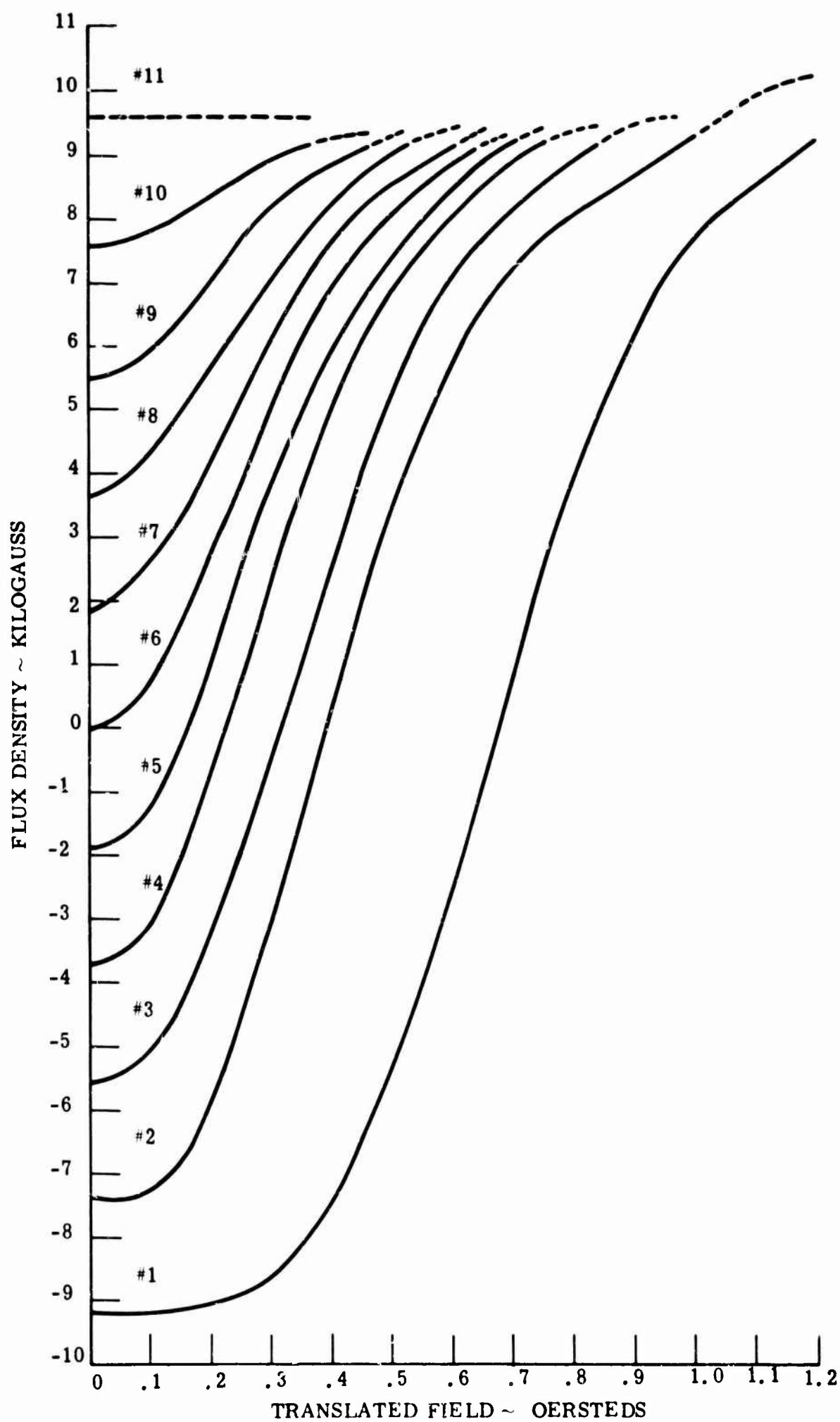$$H_e = 0.436 - 0.144 B + 0.0175 B^2 , \qquad (3)$$

Figure 4-5. Fitted Polynomials

was fitted to the last three points in Table 4-1. Figure 4-6 is a plot of the magnetization curve plotted from Table 4-1. A portion of the extrapolating parabola is shown as a dashed curve in this figure. It will be noted that the abscissa is the external field, H_e. It is easy to show algebraically, with the use of Equation (1), that if H_e is a second-degree polynomial in B, then H_i is also. Thus equivalent results would have been obtained if the extrapolation had been done in terms of H_i.

To allow some margin, the stretching factor for flux density was taken as 1.15. This brings the 8-kilogauss peak value to 9.2 kilogauss. The corresponding value of H_e from Equation (3) is 0.5924 oersteds. The ratio of the former 0.405 oersted value to this number is

$$C = \frac{0.405}{0.5924} = 0.68366 . \tag{4}$$

This is the reciprocal of the stretching factor for the magnetic field values.

The new polynomial corresponding to Equation (2) is then

$$B_S = \sum_{j=1}^{8} A_{jS} H_S^{j-1} , \tag{5}$$

where the subscript S indicates the stretched curves. This subscript is dropped later. The new coefficients for the polynomial were found from

$$A_{jS} = 1.15 \, C^{j-1} A_j . \tag{6}$$

Equation (6) was applied to the coefficients of each of the eleven reference curves of Figure 4-5. The results were used as the input reference curves for the computer program.

4.3.1.3 Interpolation Scheme

An examination of the curves of Figure 4-5 shows that interpolation with a constant interpolation coefficient is not realistic. Curve 5 may be used as an example. Suppose that this curve were not available, and it was required to obtain it by interpolation. The interpolation coefficient is the ratio of differences between appropriate ordinates,

$$k_3 = \frac{B_5 - B_3}{B_7 - B_3} , \tag{7}$$

where the subscripts refer to the curve numbers. Having the curve 5 available, one may obtain the interpolation coefficient, k_5, as a function of the abscissa (translated magnetic field). This function is plotted in Figure 4-7. The beginning point value is one-half, and for low values of the abscissa, k_3 remains nearly constant at this value. It then gradually rises in value. Over the right-hand portion of the curve, the points seem erratic. This has been attributed to instrument errors in the original data, inaccuracies in the reading of the graphs, and the high sensitivity of the coefficient to these errors in this region of the curves.

The scheme to be used for interpolation in the main program should take into account the general shape of the curve in Figure 4-7, and yet the scheme must be fairly simple. The requirements of the main program are that a BH curve be derivable from the coordinates of its end points, together with the use of the eleven stored reference curves. It is evident that the interpolation coefficient must generally have a value at the end point of the interpolated curve different from the value at the beginning point. In the program, the beginning point value, H_{KAI}, and the end point value, H_{KCI}, are found from the equivalent of Equation (7), using the flux density at the beginning or end point, as appropriate, in place of B_3. The coefficient at any intermediate point is then taken as a parabolic function of the abscissa,

$$H_{KLI} = H_{KAI} + X^2 (H_{KCI} - H_{KAI}).$$
(8)

where X is the ratio of the abscissa to its total range. Therefore X varies from zero to one over the range of the derived curve. It is easily verified that Equation (8) satisfies the beginning and end point requirements, and has a zero slope at the beginning point. Such a function was considered to best meet the requirements of simplicity with a shape similar to that of Figure 4-7.

The scheme was tested by applying it to one of the Allegheny Ludlum curves. The curve tested is the longest descending branch of a minor loop illustrated in Figure 4-4. This curve was selected because it has a greater range than any of the other corresponding curves in its set. The actual curve was inverted about the origin to make it ascending, translated, and replotted in Figure 4-8. The curve obtained by interpolation between reference curves 4 and 5 is shown dashed in Figure 4-8 for comparison. The discrepancy is believed to be comparable to the instrument and other errors.

4.3.2 Alternate Methods Which Appear Applicable

Several methods of fitting BH curves with analytical functions and of interpolating between such curves were investigated. One of the curve-fitting methods, described later, was tried and found successful but not used, because the seventh degree polynomial is simpler.

The problems fall into two distinct areas, curve-fitting and interpolation. Interpolation methods are divided into three classes. The first of these is interpolation between sets of curves corresponding to various peak values of end points of the major hysteresis loop, such as the 2, 4, 6, and 8 kilogauss sets of curves obtained from Allegheny Ludlum. The second is interpolation between the curves in any such set, that is, the generation of additional curves. The third is the type of interpolation that is suitable for use in the digital simulation, that is, a scheme which will generate a curve from the coordinates of its end points, under the conditions of an arbitrary history, and using a limited amount of input information derived from the original BH curves. Only the first two types of interpolation are discussed in this section. The third type was discussed in Section 4.3.1.
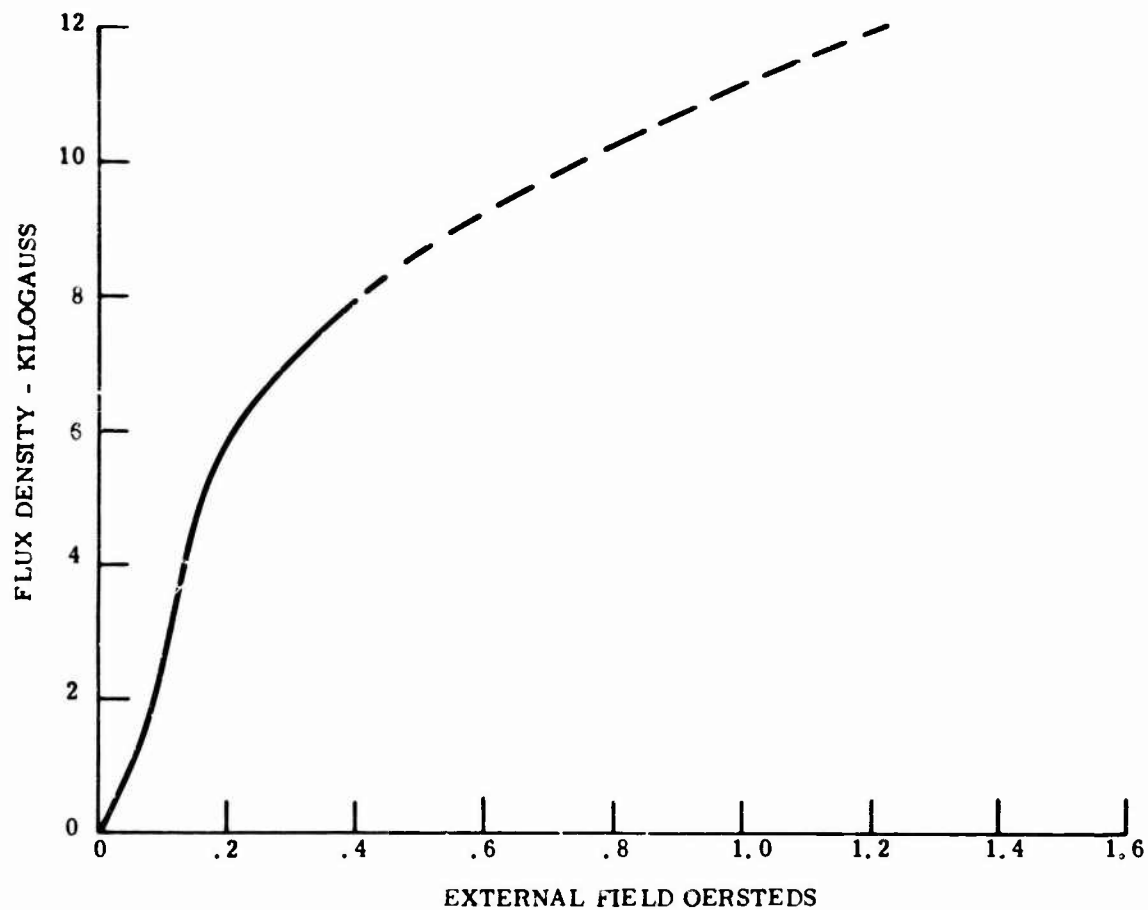
Figure 4-6. Magnetization Curve and Extrapolation Parabola
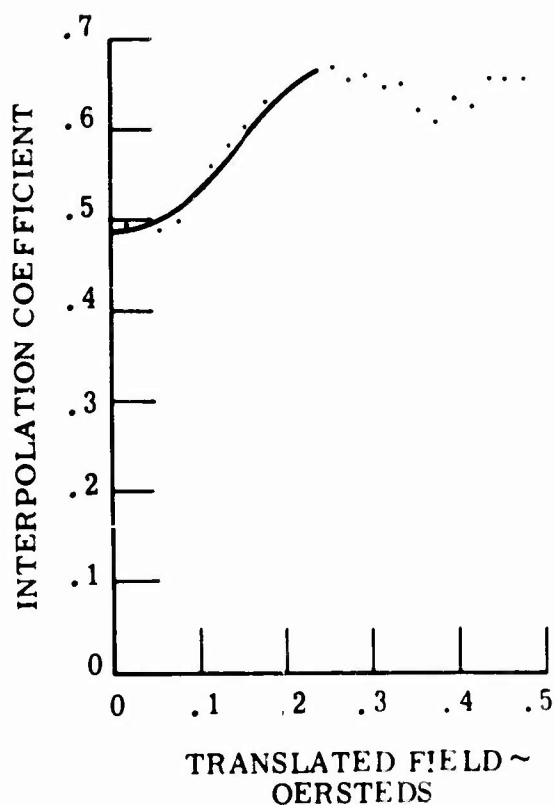

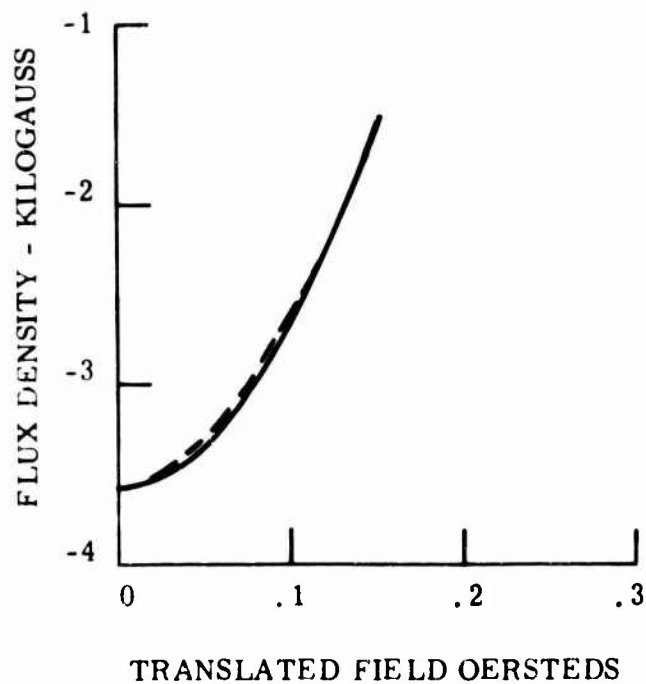Figure 4-7. Interpolation Coefficient

Figure 4-8. Comparison of Actual
and Interpolated Curves

This section will discuss curve-fitting in general, then fitting magnetic hysteresis curves in particular, and finally the various types of interpolation.

4.3.2.1 Curve-Fitting By Interpolation Techniques

The most familiar form for fitting a curve

$$y = f(x), \tag{1}$$

is by means of polynomials $P(x)$. These are generally chosen as "interpolation" polynomials, that is so as to pass through n points of the curve (1), generally equally spaced over the interval over which the fit is desired, the degree of the polynomial being one less than the number of fitted points, so that it has as many constants (coefficients) as the number of points. If the fit is not too good between the points, then one increases the number of fitted points as well as the degrees of the polynomial. Occasionally it happens that even this does not help, and as the number of fitted points increases, the discrepancies between $f(s)$ and $P(x)$ between the x_i also increase. This is likely to happen when the curve (1) has both flattish and steep portions.

Some of these difficulties may be avoided by using other forms for the curve-fitting components. In particular, we consider approximations of the form

$$f(x) \sim \sum_i A_i / \left[(x-x_i)^2 + B^2 \right] = \sum_i A_i R(x-x_i), \tag{2}$$

where x_i are equally spaced, a distance Δx apart over the interval in question, and B is a predetermined constant. The A_i are chosen so that the right-hand member of (2) agrees with $f(x)$ at the points x_i.

If the constant B is small compared with Δx, then

$$R(0) = \frac{1}{B^2} \tag{3}$$

is large, and $R(x)$ falls off rapidly, being equal to $1/\left[B^2 + (\Delta x)^2 \right]$ at $x = \Delta x$. Therefore each coefficient A_i in (2) is approximately proportional to the local ordinate $f(x_i)$. While this gives one an immediate estimate for the constants A_i and their variation with the shape of $f(x)$, it has the disadvantage that between the points x_i the right hand member of (2) decreases to numerically small values. Thus the right-hand member of (2) has the appearance shown schematically in Figure 4-9. On the other hand, if B is much larger than Δx, then the shape of $R(x)$ is rather like a parabola with a small curvature, at least for some distance to each side of its maximums. This follows from the expansion

$$R(x) = 1/B^2 - x^2/B^4 + \ldots, \qquad |x| < B. \tag{4}$$

While there is no difficulty in solving the linear equations for A_i, the variation of the coefficients with the shape of $f(x)$ is not immediately predictable.
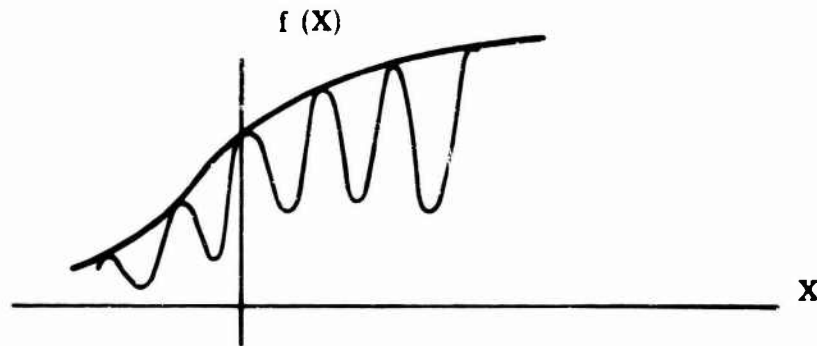
f (X)

X

Figure 4-9.

From the above it would appear that any special advantage that the form (2) might possess would be attained by having B of the same order of magnitude as Δx. It is believed that rather than choosing a large $B/\Delta x$, it is preferable to double the number of points x_i. Of course, the final decision on whether the form (2) is better than some other form of approximating functions lies in comparing the discrepancies between the true shape and the approximating shape, at points between the fitted points. A predictable and systematic variation of the coefficients A_i with the shape of $f(x)$ is also desirable, if possible.

One property of Equation (2) (and this is true for any shape $R(x)$ provided that x_i are equally spaced points), is that the matrix of the coefficients of the equations to be solved for A_i has the same elements in each diagonal parallel to the main diagonals. The matrix is also symmetric about the main diagonal, if $R(x)$ is even in x. The same statements apply to the inverse matrix.

As an alternative one may use the form (2), but choose the coefficients in some other way than by imposing an exact fit at x_i. Thus, as discussed later in Section 4.3.2.2, one may determine the coefficients in (2) by the least squares criterion, that is, so that the sum of the squares of the discrepancies between the left and the right sides of (2) at the points x_i is least. As will be shown, this gives rise to linear equations for the coefficients A_i.

The form was used to fit each of the curves in the 8-kilogauss set furnished by Allegheny Ludlum. An eleven-point fit was made by an IBM 7094 digital computer program coded in Fortran II. The equations programmed are listed in Appendix III. The runs were made for values of the ratio of $B/\Delta x$ equal to 0.25, 0.5, 1, 2, and 3. Twenty-one points were taken from each curve to be fitted, the two end points and every 0.05 of the range of H. The multiples of 0.1 of the range of H, together with the two end points, were the eleven points used for curve-fitting. The ten intermediate points were used for checking the goodness of fit. It was felt that the discrepancies between the fitted expression and the original data would be greatest at these points, which lie midway between the fitted points. The errors were least for ratios of $B/\Delta x$ equal to 1.5, 2, or 3. For any fitted curve, the ratio selected should be that which yields the least value of the maximum error. After this selection was made for each of the fitted curves, the worst error was 380 gauss.

A great deal of the above readily carries over to other shapes $R(x)$ which have a maximum at $x = 0$; are symmetric in x, and decrease to zero to either side. Several such possible shapes are

$$1/(x^2 + B^2)^n, \qquad e^{-x^2/a^2}, \qquad \text{and sech }^n(x/a). \tag{5}$$

If $R(x)$ is chosen as indicated in Figure 4-10, then (2) reduces to a polygonal approximation to $f(x)$ obtained by drawing straight line segments between the points of (i) corresponding to equally spaced ordinates.
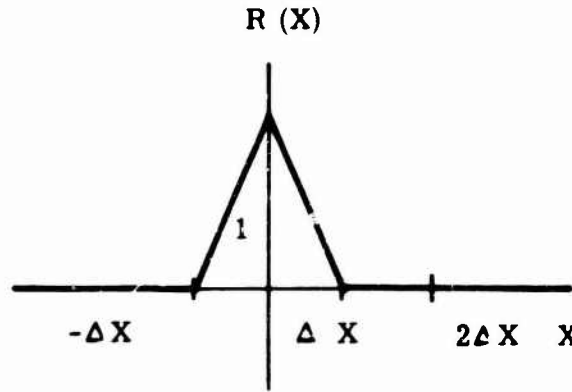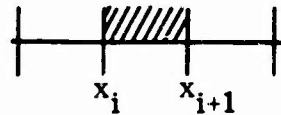

Figure 4-10.

This requires merely storage of the ordinates $f(x_i)$ and linear interpolation between them. It is too rough for high accuracy, but quadratic interpolation based on interpolation using several adjacent ordinates may be very effective.

For

$$x_i = i(\Delta x) < x < (i+1)\ \Delta x = x_{i+1} \tag{6}$$

where neither x_i nor x_{i+1} is an end point. The interpolation is given by the interpolation polynomial fitting the values of $f(x_i)$ at $x = x_{i-1},\ x_i,\ x_{i+1}\ x_{i+2}$:

$$f(x) = m_0\ f(x_{i-1}) + m_1\ f(x_i) + m_2\ f(x_{i+1}) + m_3\ f(x_{i+2}) \tag{7}$$

where $m_0,\ m_1,\ m_2,\ m_3$ are given by

$$m_0 = -\frac{(x-x_i)\ (x-x_{i+1})\ (x-x_{i+2})}{(\Delta x)^3\ 1 \cdot 2 \cdot 3} = m_0\ (x) = -\frac{\theta(\theta-1)(\theta-2)}{3!}$$

$$m_1 = \frac{(x-x_{i-1})\ (x-x_{i+1})\ (x-x_{i+2})}{(\Delta x)^3\ 1 \cdot 1 \cdot 2} = m_1\ (x) = \frac{(\theta+1)(\theta-1)(\theta-2)}{1!2!}$$

$$m_2 = m_1\ (x_i + x_{i+1} - x)$$

$$m_3 = m_0\ (x_i + x_{i+1} - x) \tag{8}$$

where

$$\theta = \frac{x-x_i}{\Delta x} \tag{9}$$

If x_i or x_{i+1} is an end point, then one-sided interpolation may be used in place of (7). Thus in $x_0 < x < x_0 + \Delta x$ Equation (7) holds, but with one sided values. Thus for $x_1 < x < x_2$

$$f(x) = m_0 \, f(x_2) + \dots$$

$$m_0 = - \frac{(x-x_1)(x-x_2)(x-x_3)}{3! \, (\Delta x)^3} = - \tag{10}$$

These can also be expressed in terms of first, second, and third finite differences.

4.3.2.2 Curve-Fitting by Least Squares Techniques

Let $f(x)$ be a given function of the independent variable x over a proper interval (a, b). We are concerned with approximating to $f(x)$ by means of a linear combination of given functions:

$$f(x) \sim C_1 f_1(x) + C_2 f_2(x) + \dots + C_k f_k(x), \tag{1}$$

where $f_1, f_2, \dots$ are functions of x only, and the C_i are constants to be chosen so that the "errors" at n prescribed points

$$x_1, x_2, \dots, x_n \tag{2}$$

are least in the sense that the sum of their squares is smaller than for any other set of coefficients C_i in (1).

It is evident that unless the number n of points in (2) is greater than the number k of terms on the right of (1), the errors can be made to vanish (provided that the determinant $\left| f_i(x_j) \right|$ does not vanish), and the least square fit reduces to an interpolation fit.

By a linear change of variable the interval (a, b) can be transformed into the interval $(0, 1)$, and this we assume to be the case in the following. The points (2) will then lie in $(0, 1)$. They may include one or both of the end points.

The quantity to be minimized is thus

$$Q = \sum_{i=1}^{n} \left(\sum_{j=1}^{k} C_j f_j(x_i) - f(x_i) \right)^2 . \tag{3}$$

Evidently, Q is, in general, a definite (that is a positive) quadratic form in the coefficients C_j. It takes on its minimum at the values of C_j which satisfy the k equations

$$\frac{1}{2} \frac{\partial Q}{\partial C_\ell} = 0 = \sum_{i=1}^{n} \sum_{j=1}^{k} \left[C_j f_j(x_i) - f(x_i) \right] f_\ell(x_i); \ell = 1, \dots, k \tag{4}$$

Rearranging the terms results in k linear equations,

$$\sum_{j=1}^{k} C_j \left[\sum_{i=1}^{n} f_j(x_i) \cdot f_\ell(x_i) \right] = \sum_{i=1}^{n} f(x_i) f_\ell(x_i); \ell = 1, \dots, k \tag{5}$$

In these equations C_j are the unknowns, while the coefficients of these unknowns are sums of products of the functions f_j at the points (2), and the right-hand constants are sums of products of the values of the left-hand member of (1) by the values of the functions f_j, all evaluated at respective values of the points (2) chosen properly in each factor. The solution of these equations, when substituted in the right-hand side of (1), yields the least square fit for $f(x)$.

An example is that in which the functions f_i are polynomials:

$$f_j(x) = x^{j-1}, \tag{6}$$

Then Equations (5) reduce to

$$\sum_{j=1}^{k} C_j \left[\sum_{i=1}^{n} x_i^{j-1} x_i^{\ell-1} \right] = \sum_{i=1}^{n} f(x_i) x_i^{\ell-1}; \; \ell=1, \ldots, k \tag{7}$$

The least square approximation in general will not yield a perfect fit at the points (2). In particular, if the end points are included among the points (2), it is not to be expected that the least square fit will yield the exact values of $f(x)$ at these points either. If it is desired to obtain an exact fit at these points, say for polynomial fits, then one proceeds as follows.

We choose for the polynomials the functions

$$f_j(x) = x(1-x) x^{j-1} \tag{8}$$

thus replacing (1) by

$$f(x) \sim x(1-x) \left[C_0 + C_1 x + C_2 x^2 + \ldots + C_k x^k \right] = \sum_{j=0}^{k} C_j \left(x^{j+1} - x^{j+2} \right) \tag{9}$$

where, with a slight change of notation, the subscript has been allowed to range over 0 as well. The form (9) automatically vanishes at the end points $x = 0$ and $x = 1$.

As an alternative method, one may, before applying least squares, subtract from $f(x)$ a linear function of x which takes on at the end points the same values as $f(x)$. Then one proceeds to apply least squares to the resulting difference. We shall assume in the following that this has been done, and will use $f(x)$ for the difference function. With this in mind, Equations (5) apply and, more explicitly, yield

$$\sum_{j=1}^{k} C_j \left[\sum_{i=1}^{n} x_i^2 (1-x_i)^2 x_i^{j+\ell} \right] = \sum_{i=1}^{n} \left[f(x_i) x_i (1-x_i) x_i^{\ell} \right]; \; -\ell=1, \ldots, k. \tag{10}$$

Another alternative is to divide both sides of (9) by $x(1-x)$ and choose a polynomial represented by the bracketed factor in (9) so that it fits $f(x)/x(1-x)$ in the least squares sense.

The resulting coefficients C_j will not be the same as above. There will also be the difficulty of obtaining limits of indeterminate forms when evaluating the function

$$\frac{f(x)}{x(1-x)} \tag{11}$$

at the end points.

Least square methods can be readily extended to the case where the squares of the deviations are weighted with weights w_i which are prescribed with the position x_i.

It is believed that, as compared with an interpolation polynomial which takes on the values $f(x_i)$ at x_i, the least square polynomials have an over-all smaller error over the whole interval, say when x_i are equally spaced. The error of the interpolation polynomial can be expressed in terms of the $(n+1)$th derivative of $f(x)$; no estimate of the error of the least square approximation polynomial is known.

4.3.2.3 Curve-Fitting of BH Curves by Inversion

Examination of the hysteresis curves and of the curves obtained by reversing the sign of dH/dt, at $H_R = H_{R,1}$, $H_{R,2}$, ... shows that, after reversal, the new curve resembles the "inverted image" of the preceding curve segment, obtained by turning the latter through 180°, about the midpoint of the line segment joining its end points. This is exactly true for the ascending branch of the major loop, which is obtained from the descending one by rotating the latter 180° about the origin H=0, B=0, which is the midpoint of the line segment joining H_m, B_m to $-H_m$, $-B_m$. It is also true within very high accuracy for any rank curve and the curve of the following rank, if $H_{R,i}$ and $H_{R,i+1}$ are close, whereupon the curve segment between these reversal points is a parabola, and so is its inverted image. For the curves of rank i, i > 1, if the end points $H_{R,i}$, $H_{R,i+1}$ are far apart, and B_m is large enough so that the hysteresis curve has a point of inflection and appreciable reversed curvature, it is true only in the neighborhood of the reversal point. Thus on Figure 4-11 if, after descending along the main hysteresis curve from the vertex A to the point B, H starts increasing, then the path followed is BCA. The inverted path is BC'DA. Near B the two paths lie close to each other, but they deviate for larger H.

The curve BCA passes through A, the previous reversal point, and this is in accordance with the general rule for the curves of rank i, that they aim for the previous reversal point, and if continued beyond (for i > 1), follow along the curve of rank (i-2).

The inverted curve BC'DA also passes through the previous reversal point A, since in rotating through 180° about the midpoint the end points are interchanged.

If a curve has the equation
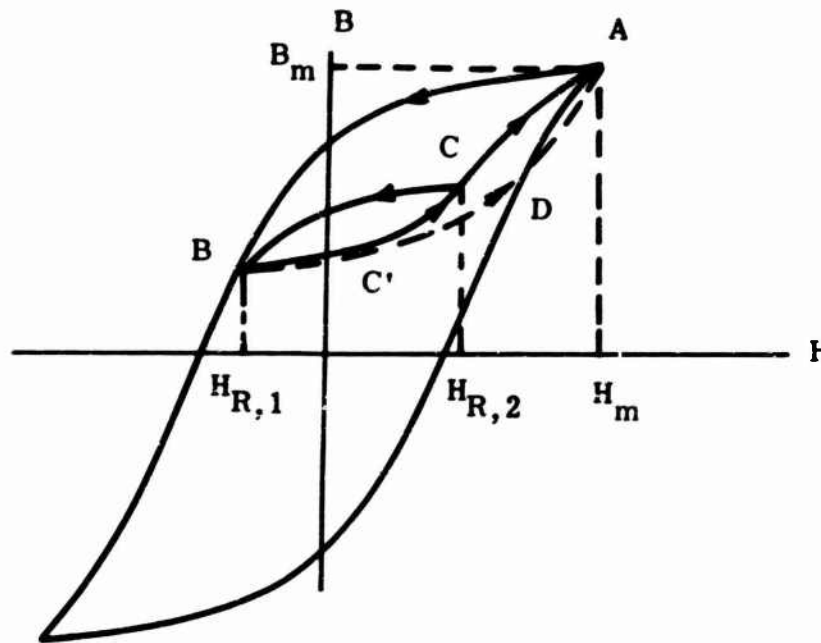
$$B = f(H), \quad H_{R1} < H < H_m, \tag{1}$$

Figure 4-11.

then the inverted image between these points is given by

$$H + H' = H_A + H_{R1}, \qquad B + B' = f(H_A) + f(H_{R1}), \tag{2}$$

where half of the right hand members yield the coordinates of the midpoint of the straight line segment between the end points, and H', B' denote the point which is obtained by inverting the point H, B. Hence, in equation form, the inverted curve is given by

$$B' = f(H_A) + f(H_{R1}) - f(H) = \text{where } H = H_A + H_{R1} - H'. \tag{3}$$

Eliminating H, and then dropping the primes,

$$B = f(H_A) + f(H_{R1}) - f(H_A + H_{R1} - H). \tag{4}$$

With proper changes of notation the form (3) can be used to derive the curves of rank i from those of rank $i-1$, where the latter are obtainable by inversion of the preceding ones.

Where an inverted curve differs appreciably from the reversed curve, the correction to be added to the right-hand member of (3) (or of the corresponding equation for the curve of rank i) must be a function of H which vanishes at the two end points. This function increases numerically very slowly at B on Figure 4-11, or near its first reversal point, while it approaches its following reversal point more steeply. We proceed to derive several forms of functions having this property. For definiteness, we change the independent variable to the normalized variable x, and suppose that the roots are at $x=0$, $x=1$, with $x=0$ as the root with the slow numerical increase.

A simple function having the desired properties is given by

$$y = C x^2 (1-x). \tag{5}$$

This has a vanishing slope at x=0, and would do only if the two curves (the reversed and inverted curves) are tangent to each other at the reversal point.

Another possible function is given by

$$y = C x (e^{-\beta x} - e^{-\beta}), \quad \beta > 0, \tag{6}$$

where β and C are constants. The ratio of slopes at x=0 and at x=1 is numerically equal to

$$(e^{\beta} - 1): \beta. \tag{7}$$

This ratio can be made as large as desired by choosing β large enough. By replacing x by (1-x) in (6), the small slope can be made to occur at x=0, and the large one at x=1.

Additional functions with the desired properties can be obtained by starting with a function like

$$y = f(x) = J_n(x), \quad n = 2, 3, \ldots, \tag{8}$$

whose appearance between x=0 and the first positive root is as shown schematically in Figure 4-12, with a zero slope at x=0. To obtain from (8) a function with a small positive slope at the left end, one cuts the curve with a line

$$y = \epsilon, \tag{9}$$

obtaining two roots $x=x_1$ near zero, $x=x_2$ with a small slope at x_1. By replacing x by

$$\xi = (x-x_1)/(x_2-x_1) \tag{10}$$

one shifts the roots to $\xi = 0$, $\xi = 1$.

Figure 4-12.

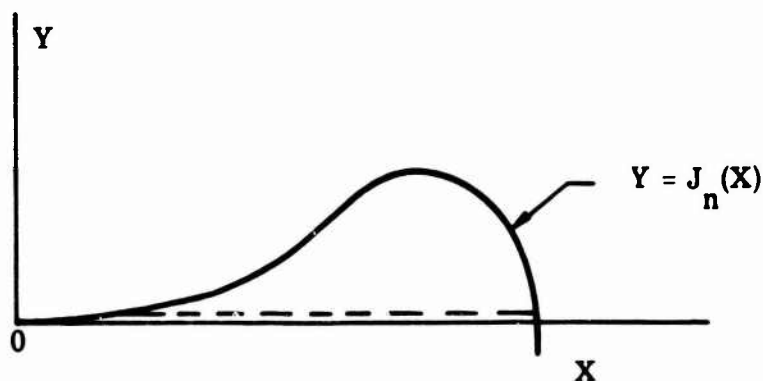The solution of (8), (9) may have to be carried out by a trial-and-error or by a successive improvement method. However, one may choose x_2 as a value in the table and near the root. Then $\epsilon = f(x_2)$ is known, and presumably small. The value x_1 can then be determined by using the first term of the power series expansion,

$$J_n(x) = \frac{x^n}{2^n n!} (1 - \ldots) = \epsilon. \tag{11}$$

4-38

The precise f(x) to be used for ΔB, for the family of 2nd rank (H, B) curves, and the variation of f(x) with H_{R1} and with H_m, requires a great deal of trial and error.

4.3.2.4 Differential Equation for the Second-Rank Hysteresis Curves

A family of curves such that one and only one curve passes through every point of a certain region of the (x, y) plane, can be described by means of its differential equation

$$\frac{dy}{dx} = F(x, y), \tag{1}$$

where F(x, y) is the slope of the curve passing through (x, y). This equation yields the curves themselves only if one carries out an integration of (1), either analytically, or numerically.

In the following, an attempt will be made to obtain a differential equation of the form

$$\frac{dB}{dH} = F(H, B). \tag{2}$$

for representing the curves of rank 2, that is the curves obtained after one has descended along a particular hysteresis curve to a point H_R, then increased H to H_m, the value of H at the vertex of the hysteresis curve. The starting points of these curves are the points of the descending branch of the hysteresis curve. These curves are shown in Figure 4-13.
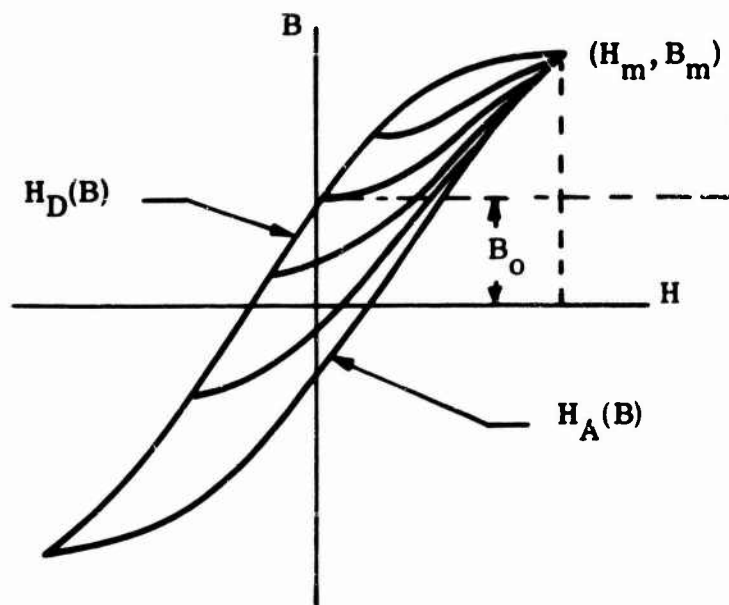
Figure 4-13.

Examination of the curves of Figure 4-13 shows that along any horizontal straight line

$$B = \text{constant} \tag{3}$$

The slopes increase from a small value m_1 to the value m_2 which is the slope of the ascending branch of the hysteresis curve through the point with the constant B in question. The value m_1, it follows from the inversion properties explained in Section 4.3.2.3, has the same slope as the slope of the descending hysteresis curve at its vertex (H_m, B_m).

Thus m_1 is independent of the right hand constant in (3), depending only upon H_m. In fact, on the Allegheny Ludlum (H, B)-curves m_1 appears to be zero, or even slightly negative. This, however, can never actually be the case with any magnetic material, and must be due to an instrument error.

If, for simplicity, we do assume that m_1 vanishes, then a possible simple form for (2) is given by

$$\frac{dB}{dH} = \theta \, m_2 \; ; \tag{4}$$

where θ is the fractional distance along the line (3) from the left, to the total length of this line:

$$\theta = (H - H_D)/(H_A - H_D), \tag{5}$$

where

$$H_A = H_A(B), \qquad H_D = H_D(B), \tag{6}$$

are the equations of the ascending and the descending branches of the hysteresis curves respectively. It follows that

$$m_2 = 1/dH_A/dB = 1/H_A'(B). \tag{7}$$

Substitution from (5), (7) into (4) yields the differential equation

$$\frac{dB}{dH} = \frac{H - H_D(B)}{H_A(B) - H_D(B)} \; \frac{1}{H_A'(B)} \tag{8}$$

If m_1 is not negligible, then (4) must be modified, say, into

$$\frac{dB}{dH} = (1-\theta) \, m_1 + \theta \, m_2 \tag{9}$$

Utilizing (5) and (7) one adds to the right-hand side of (8)

$$m_1 \; \frac{H_A(B) - H}{H_A(B) - H_D(B)} \; . \tag{10}$$

By utilizing the inversion properties of the two hysteresis branches one may express H_D in terms of H_A, as follows:

$$H_D(B) = -H_A(-B) \tag{11}$$

Whether (8) or the modified form with (10) added on fits the curves of Figure 4-13 can be determined by a numerical comparison of the actual slopes of the curves with those computed from the equations, or better yet, by integrating these differential equations

and comparing the resulting curves with the curves of Figure 4-13. The analytic integration off-hand appears difficult. The numerical integration, if it is used, has to be carried out with high accuracy.

Various changes in (9) are possible and may be desirable if (9) does not yield a good fit. Thus, one may replace θ by any function of θ, $g(\theta)$ which has the property that it increases with θ, vanishes for $\theta = 0$, and is equal to 1 for $\theta = 1$. Moreover, $g(\theta)$ may vary with the height of the line of constant B.

A further alternative consists in fitting slopes along vertical, rather than horizontal, lines in Figure 4-13. Along a vertical line, it will be seen that, as B increases, the slope starts with the slope m_2 of the ascending branch of the hysteresis curve for the constant value of H in question and decreases to m_1 at the intersection with the descending branch. One may use (9), but θ defined by

$$\theta = (B-B_A)/(B_D-B_A), \tag{12}$$

where B_A, B_D represent the ascending and descending branches, with B expressed in terms of H, and

$$m_2 = dB_A/dH = B_A'(H) \tag{13}$$

There results

$$\frac{dB}{dH} = \frac{B_A'(H)[B-B_A(H)]}{B_D(H) - B_A(H)} + m_1 \frac{B_D(H) - B}{B_D(H) - B_A(H)}. \tag{14}$$

This is linear, but not homogeneous, in B, with coefficients which are functions of the independent variable H. Such a differential equation can be integrated by means of quadratures, and for this reason (14) would be preferable to (8) and its two consequent equations. However, the linear variation of slope with distance appears to be questionable along vertical lines in Figure 4-13. Hence replacement of θ by $g(\theta)$, a function of θ, may be necessary. This would lose the linearity property of the differential equation.

While the use of differential equations in describing the (B, H)-curves is an added complication, to be avoided if the explicit equations for these curves can be obtained, it may be said, that, from the point of view of integrating for the motion of a satellite and its orientation along its orbit, the number of degrees of freedom is already high, and the use of (8) or (14) only increases by 1 the order of the system. What is a more serious item is the fact that the differential equations proposed have only been considered for the second rank (H, B) curves. For third, and higher rank curves, which depend upon several preceding reversal values of H as well, the form (2) is insufficient and either a higher order system is needed or a way of describing the changes in F upon reversal (of the sign of dH/dt).

It may be added in conclusion that from a scientific point of view, it would be very desirable if a way of describing magnetic properties of ferromagnetic materials based on some theory, were worked out by physicists, from which, starting with the established tenet that elementary magnets have a constant moment, and all the magnetic properties are due to the orientation of these elementary (atomic or molecular) magnets, one could predict the magnetic behavior of a magnetic material, once its chemical and metallurgical structure is known. The work by Ewing of a model based on a collection of regularly arranged collection of small magnets, raised hopes that this may be possible, but to date the task has proved too difficult, though the nature of the elementary magnets has indeed been clarified in terms of quantum theory, Bohr magnetons, and electron orbital spin. It is possible, that when this theory is worked out, it will be in the form of differential equations resembling (2). A review of Neel's theory and other theoretical attempts in the booklet by G. F. Brown shows that theory is still a long way from theoretical explanation of properties of magnetic materials. Possibly some semi-empirical theory, with the inclusion of some sort of "frictional" energy dissipation accompanying (H, B) changes might be developed in the meantime.

4.3.2.5 Interpolation of Second-Rank BH Curves

For a given hysteresis loop between the points (H_m, B_m) and $(-H_m, -B_m)$, second rank (H, B) curves are available, proceeding from five points of the descending branch corresponding to values of B_R differing by

$$B = \frac{2}{5} B_m \tag{1}$$

and corresponding to

$$B = B_m, \ (3/5) B_m, \ (1/5) B_m, \ -(1/5) B_m, \ -(3/5) B_m, \ - B_m, \tag{2}$$

where the last curve is the ascending branch of the hysteresis loop and forms a limiting case of the second rank curves. These curves start at values of H denoted by H_R (corresponding to reversal of sign of dH/dt) and all proceed to the point (H_m, B_m).

The question is that of interpolation between the above curves.

One method is that of linear"slanting" interpolation. This consists in replacing the descending hysteresis curve by straight lines between adjacent starting points of the second rank curves, as shown schematically on Figure 4-14 at $P_0 P_1$. This line segment $P_2 P_1$ is continued past P_1 until it meets the vertical line $H = H_m$ at a point Q_1. Then many line segments are drawn between the second rank curves through P_1, P_2, all proceeding from Q_1. The interpolated curves are obtained by dividing these segments in a constant ratio. On Figure 4-14 the mid-points on five such line segments have been indicated. A curve passing through these points is the interpolated curve corresponding to an initial point $P_{1.5}$ corresponding to H_R midway between H_R of P_1 and P_2.
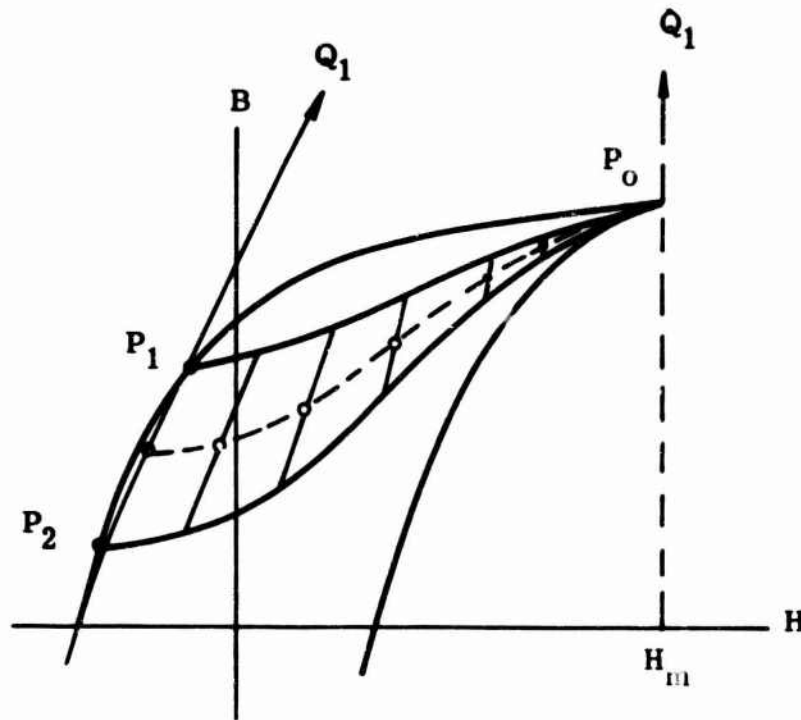
Figure 4-14.

It also corresponds to a B-value midway between those of P_1 and P_2. Thus the starting point does <u>not</u> lie on the descending branch proper, the discrepancy being large where the curvature of the hysteresis curve is appreciable.

Each segment P_0P_1, P_1P_2, ... cuts the vertical through P_0 in a separate point $Q_0(=P_0)$, Q_1, Q_2, ... The discrepancy in the top-most interval is most severe.

An improvement in the above procedure consists in replotting the original second rank curves so that they start at points on a vertical axis and stretching each one horizontally in a proper ratio so that they end in the same point. The resulting diagram is shown schematically in Figure 4-15, where the B axis has the same scale as in Figure 4-14, and the variable x is given by

$$x = \frac{H - H_R}{H_m - H_R} \tag{3}$$

and runs from 0 to 1 for <u>each</u> second rank curve. The ratio of scales is given by the factor

$$f = H_m - H_R \tag{4}$$

and this is plotted on Figure 4-16.

The second rank curves on Figure 4-14 are obtained by multiplying each curve of Figure 4-15 by the factor f of Figure 4-16 lying at the same B as the <u>starting</u> point of Figure 4-16 and transposing it to Figure 4-14 parallel to the H axis.

Figure 4-16 has the same shape as the upper descending branch of the hysteresis curve of Figure 4-14 except for being reflected in a vertical axis. If f were plotted to the left, the curve of Figure 4-16 would be congruent to that of Figure 4-14.
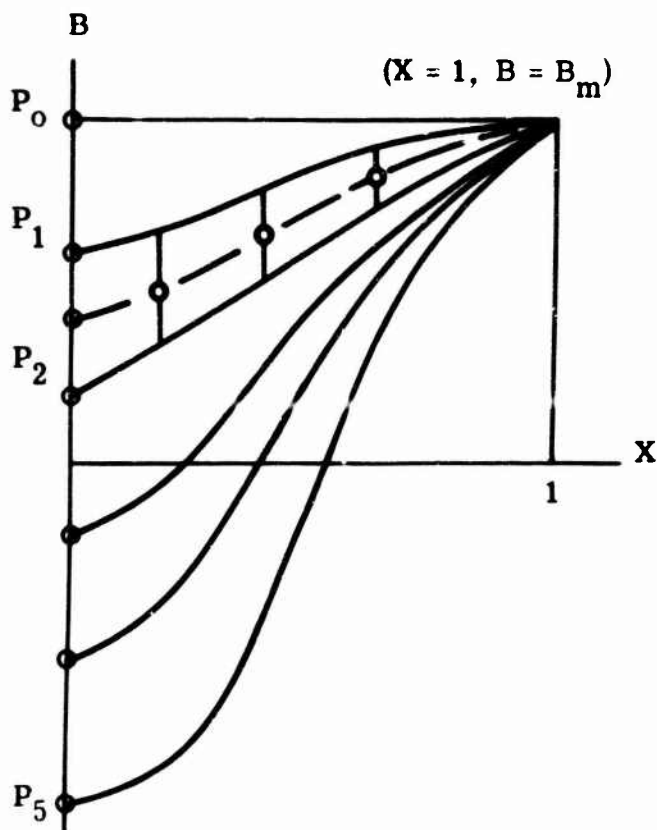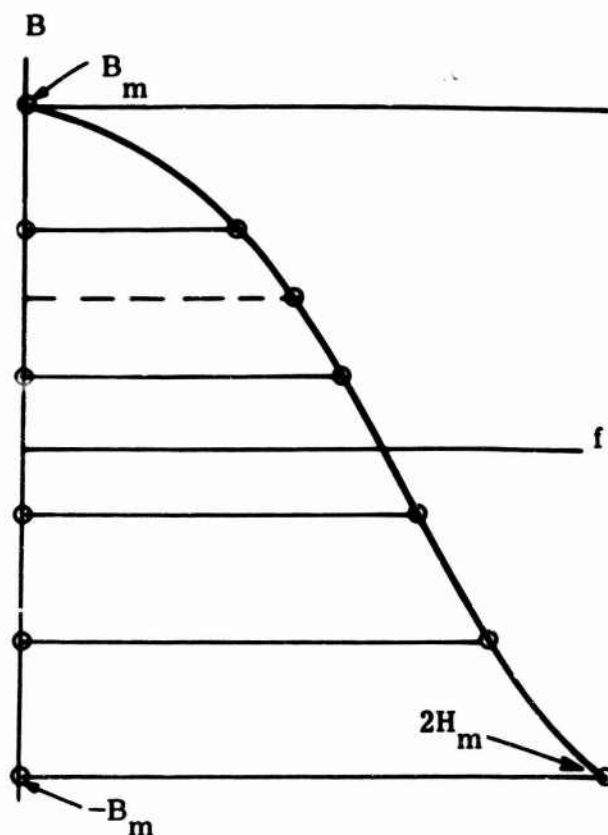
Figure 4-15.

Figure 4-16.

On Figure 4-15 the interpolation is curved out along vertical segments, as indicated schematically between the curves through P_1 and P_2. Again, the midway value is shown, as well as the curve (broken) passing through these midway values. After this curve is obtained, it is stretched horizontally by the value of f corresponding to the initial B.

The advantage of the above method over that of Figure 4-14 is that one may fit f(B) in Figure 4-16 as a function of B by means of French curves or by means of an analytic expression, say, passing through as many points as desired, since this curve, as indicated above, is derivable from the (descending branch of the) hysteresis curve.

If the curve of Figure 4-16 is replaced by straight line segments through the values (2) of B, then the method of Figure 4-15 (and the modified Figure 4-16) becomes identical with that of Figure 4-14. This procedure is _not_ recommended.

The curve fitting of Figure 4-16

$$f = f(B), \qquad H_m - H_R = f(B), \qquad H_R = H_m - f(B), \tag{5}$$

should yield H_m as a function of B and not the other way around. This is advisable in addition to the fitting of the hysteresis branch in the form

$$B = \text{function of } H = g(H) \tag{6}$$

where g is the function inverse to the $H_m - f(B)$. It is, of course, possible to solve (6) by a successive approximation method or trial and error for the H values corresponding to prescribed B-values, then identifying H with H_R in (5), obtain $f = H_m - H$.

The hysteresis curves of rank one, and the curves of rank 2 are available only from recording pen tracings of the magnetic instrument, and exhibit "wobbles" and other irregularities that have to be corrected graphically. It is evident that the aid of a good draftsman is needed to draw the curves of Figure 4-14. When this is done on graph paper with small squares, many points of Figure 4-14 can be read off and the values of B and H tabulated for the descending hysteresis branch and the four second rank curves. From the H values one can calculate x values and plot the curves of Figure 4-15.

It is planned to fit the curves of Figure 4-14 (first and second rank curves) with equations of the form

$$B = f(H, H_R) \quad \text{or} \quad B = f(H, B_R) \tag{7}$$

From these, analytic forms can be obtained for the curves of Figure 4-15, giving B as functions of x (and the starting point B_R). Suppose that the form of the equations is

$$B = \sum_k A_k (B_R) f_k (X) \ . \quad 0 < x < 1, \tag{8}$$

where the shapes of f_k are given and are the same for all the five values (2) and A_k are constants depending on the curve. For instance, if $f_k(X)$ are powers of x, the equations (8) constitute a polynomial fit.

Then the interpolation between the curves of Figure 4-15 can be carried out by applying it to the coefficients A_k. Thus, between the curves through P_1 and P_2

$$B \left[(\theta B_1 + 1 - \theta B_2), x \right]$$
$$= \Sigma \left[\theta A_k (B_1) + (1 - \theta) A_k (B_2) \right] f_k(x), \quad 0 < \theta < 1. \tag{9}$$

If, for definition's sake, there are 10 values of k in (8) then a table of 50 coefficients $A_k (B_r)$ is all that is required, since (9) can be used to obtain the equation of any intermediate curve in terms of the two curves to each side.

In principle, it is possible to interpolate A_k not linearly as in (9), but by using a Lagrange interpolation value between three adjacent curves (or values of B_R).

While we have assumed that only second rank curves and one hysteresis curve are available, it is evident that the technique is applicable if a larger number of curves, i. e., of higher rank, were available.

A check should be made between the interpolated or predicted curve and a measured curve, specially taken for this purpose. If the check is not too good, the more complex interpolation (using say three adjacent curves, or preferably a total of nine secondaries plus one primary, and interpolation of the form (9)) should be resorted to.

4.3.2.6 Interpolation Between Major Hysteresis Curves

In Section 4.3.2.5 we discussed the interpolation of the second rank BH curves indicated in Figure 4-14. The procedure recommended there is shown in Figures 4-15 and 4-16. It is evident that this procedure can be extended to other one-parameter families of curves. As an example, we now consider the interpolation between the main hysteresis curves, or the curves of rank 1. The latter are available for 4 values of B_m,

$$B_m = 2000, \ 4000, \ 6000, \ 8000 \text{ gauss} \tag{1}$$

We consider only the descending branches, indicated schematically in Figure 4-17 with arrows. The upper end points of these curves correspond to equally spaced values of B, displayed in equation (1).

The interpolation may be carried out by introducing a change of scale for the horizontal coordinate, H:

$$x = H/H_m, \tag{2}$$

and replotting these curves in the x, B plane, where they will all proceed from x=1 to x=-1. They are shown schematically in Figure 4-18.
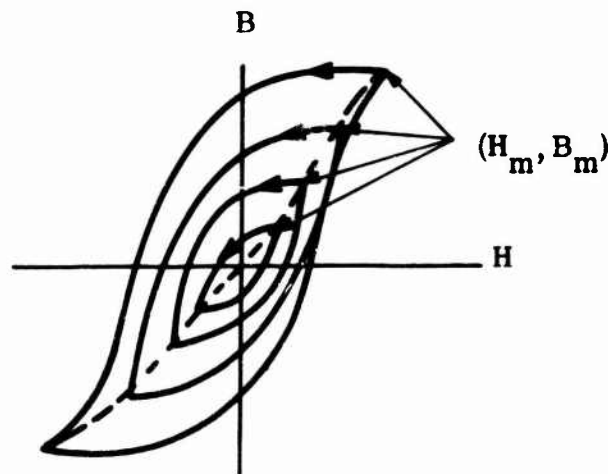

Figure 4-17.
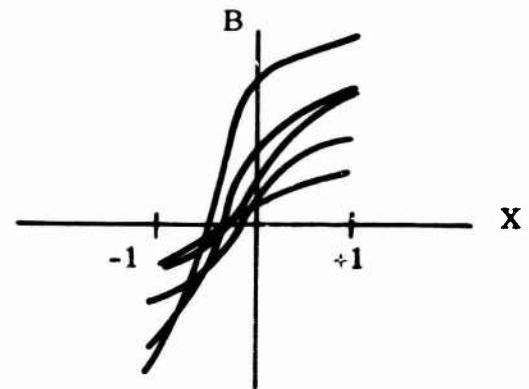
Figure 4-18.

The interpolation is carried out in Figure 4-18 by means of vertical segments joining adjacent curves. Thus, corresponding to $B_m = 7500$, these segments are divided in the ratio 3:1 with the shorter segment abutting on the $B_m = 8000$ curve. Where the two curves intersect, the interpolated point will coincide with the point of intersection, while to each side of this intersection the direction of the segment proceeding from the 6000 curve toward the 8000 curve will have opposite directions.

After a sufficient number of vertical segments and interpolated points have been obtained, the complete curve corresponding to $B_m = 7500$ is drawn through them.

To transfer the interpolated curve to the (BH)-plane of Figure 4-17, it is necessary to stretch it horizontally by the scale factor

$$s = H_m, \tag{3}$$

corresponding to the B_m value in question. Now the H_m value can be read off from Figure 4-17 by drawing the curve through the vertices of the hysteresis loops, shown as a broken line in Figure 4-18, and described by

$$B_m = B_m(H_m), \tag{4}$$

or preferably by

$$H_m = H_m(B_m), \tag{5}$$

as the abscissa corresponding to the desired B_m.

It is also possible to effect two changes of scale, one horizontal, as above, the other vertical, so that the height of the transformed curve is also fixed. Then all the vertices of the transformed curves pass through two fixed end points. The interpolation can then be carried out either horizontally or vertically. Aside from saving the extra change of scale, Figure 4-18 has the advantage that the segment of the x-axis between x=-1 and x=+1 can be included among the family of curves (it represents the origin on Figure 4-18), and used to interpolate for values of B_m less than 2000.

As mentioned in Section 4.3.2.5, it is also possible to use more sophisticated interpolation by utilizing more than the two adjacent curves in Figure 4-18.

In equation form, with rather cumbersome notation, using only linear interpolation, let the hysteresis curves be given by

$$B = B(H, B_m), \qquad B_m = B_{m,i}, \qquad i = 1, 2, 3, 4. \tag{6}$$

Then the curves of Figure 4-18 are given by

$$B = B(H_m x, \ B_m) = f(x, B_m). \tag{7}$$

The interpolated curve, corresponding to the value

$$B_m = (1-\theta) B_{m,i} + \theta B_{m,i+1}, \qquad 0 < \theta < 1 \tag{8}$$

is given by

$$B = (1-\theta) f(x, B_{m,i}) + \theta f(x, B_{m,i+1}). \tag{9}$$

The interpolated curve on Figure 4-17 is represented by

$$B = (1-\theta) f(H/H_m, \ B_{m,i}) + \theta f(H/H_m, \ B_{m,i+1}), \tag{10}$$

where H_m is obtained from Equation (5) as the value of H_m corresponding to (8).

In implementing the above on computing machines, suppose that polynomial approximations are used to fit the BH curves. Starting with polynomials of a certain degree for the (four) curves f in Equation (7) over the interval

$$-1 < x < +1 \tag{11}$$

and assuming a value of θ in (8) one carries the interpolation (9) by interpolating the respective coefficients of the polynomials. If the right-hand member of (5) is likewise approximated by means of a polynomial in B_m, then its value for B_m given by (8) is computed. On the other hand, if only its inverse function, represented by Equation (4), has been approximated (say by means of a polynomial in H_m), then it is necessary to solve for a root of (4) by some trial-and-error or successive approximation method.

Since H is known as a function of time, the representation (7) for the (BH)-curves is natural. Since this involves B_m, because the magnetic data have been taken for specified (and equidistant) values of B_m, equation (4) must be used first, assuming that H_m will be prescribed with the satellite motion. Then θ is determined from (8) and the procedure continued as outlined above.

While the procedure has been described as an interpolation between the (first rank) hysteresis curves proper, the method is obviously applicable to any one-parameter family of curves, for instance to the 2nd rank curves described in Section 4.3.2.5, and representing the B values after one has proceeded a certain distance along a particular hysteresis descending branch, then changing the sign of dH/dt by letting H increase again after it has reached a minimum at H_R. If now H increases continuously, until H has attained the upper vertex of the previous hysteresis curve, then starts to decrease again, the original (descending) branch of the hysteresis curve is followed. If, however, H increase to a value $H_{r,2}$ less than H_m, then starts decreasing, then one follows a 3rd rank curve. The second rank curves involve two parameters, in addition to H:

$$B = B(H, B_m, H_R), \tag{12}$$

and are available for a mesh of B_m, H_R values. The third rank curves are of the form

$$B = B(H, B_m, H_{R1}, H_{R2}). \tag{13}$$

They evidently involve more storage space, and must be based on time-consuming taking of data. After H has attained the maximum at $H_{R,2}$, it decreases, following (13), to a certain minimum $H_{R,3}$, then starts increasing again. If $H_{R,3}$ is greater than H_{R1}, then a 4th rank curve is followed, for which even less data is available. On the other hand, if $H_{R,3}$ is less than $H_{r,1}$, then the last portion of (13) coincides with the (6), and further reversals of sign of dH/dt can be followed for a while with the curves (12), (13).

The higher and higher rank curves, which are presumably required if H oscillates between maxima, and minima, both of which are decreasing numerically and approaching

zero, can be obtained after a while by the inversion method described in Section 4.3.2.3. As the interval between successive H_R values decreases, these curves become Rayleigh parabolas.

Opinion seems to be divided on what happens if $H_{R,2}$ proceeds to a value larger than H_{r1}. In the absence of complete data on this point, the recommendation is to proceed along the curve (4) beyond the vertex point of the original hysteresis curve, and then proceed along an outer hysteresis curve after H starts decreasing again. This may be somewhat in error, since the hysteresis curves are generally taken only after several reversals of dH/dt occurring at $\pm H_m$. The "settling down" to the final hysteresis curve occurs more quickly if H is changing at a slow rate. From this it may be presumed that the statement about picking up the new hysteresis curve may be true for slow-swinging periods (about a half hour or more).

4.3.3 Other Curve-Fitting Functions Tried and Abandoned

Several methods of fitting analytical expressions to the magnetic hysteresis curves were attempted, brought to various stages of completion, and abandoned. The functional forms tried were obtained from the literature or were modifications of such functions. Each of the forms is discussed, and, in most cases, its advantages and disadvantages are discussed. In every case, the reason for abandoning the particular form is given. This section serves not only to document the work done, but also to prevent consideration of using any one of these forms in the future, without due regard for the reason that it was rejected here.

4.3.3.1 Rayleigh Loops

Rayleigh loops are parabolas, for which B is a second degree polynomial in H. These are discussed on pages 490-491 of Reference 2. The formulas are given for loops whose end points are symmetrical with respect to the origin, but the loops are easily translated to fit other situations.

The use of a parabola allows the choice of three coefficients. These are usually forced to fit the two end points and the initial slope of the curve. This initial slope may be chosen to be that of the initial magnetization curve, or it may be a function of the flux density at which the reversal occurred. Alternatively, the three coefficients may be chosen to fit the two end points and the height, W, of a symmetrical loop, as illustrated in Figure 4-19. The attempt to fit actual magnetic curves by this method often leads to negative initial slopes.

The Rayleigh loops, based on fitting the end points and the initial slope, may yield good approximations for low values of maximum flux density. They have no inflection point, and are therefore inherently incapable of representing a hysteresis curve for which the maximum flux density even begins to approach the knee of the saturation curve. When it became apparent that flux densities beyond the inflection point would be encountered, the parabolas had to be abandoned because of this inherent limitation.
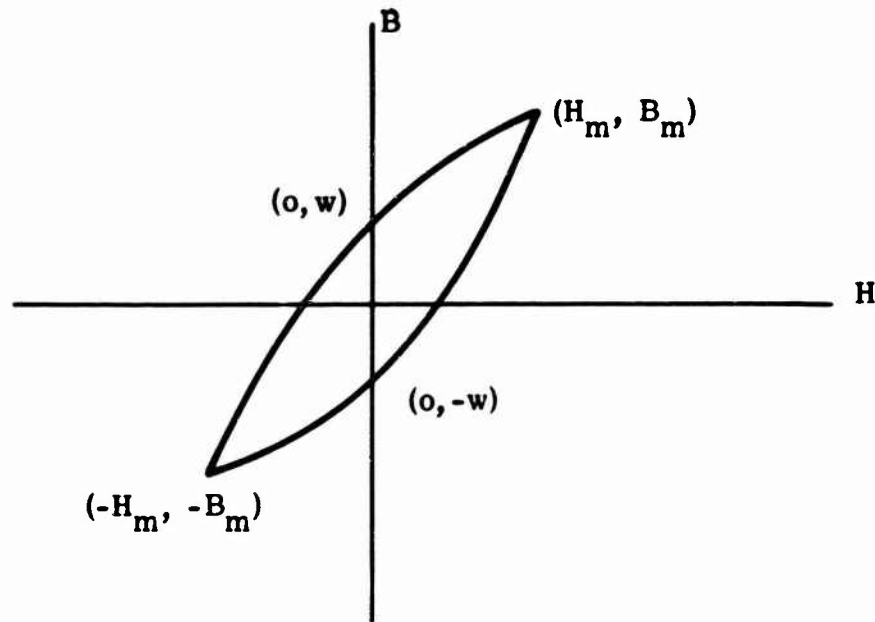
Figure 4-19.

4.3.3.2 Cubic Equations

Only cubics wherein B is a third degree polynomial in H can be considered. The use of functions wherein H is a third degree function of B might appear attractive at first glance, but in some cases B would be a multiple-valued function of H. Such a function would be an unacceptable representation of the physical curve.

When B is a third degree function of H, there are four coefficients to be chosen. These may be fitted to the two end points, the initial slope, and the height, w, of the loop formed from two symmetrical curves. This is illustrated in Figure 4-19. The upper curve is obtained by rotating the bottom one 180 degrees about the origin. The equation for the curves is

$$B = \pm W \left(1 - \frac{H^2}{H_m^2} \right) + \frac{H}{H_m} \ (3 B_m - \mu_r H_m - 2 w)$$

$$+ \frac{H^3}{2 H_m^3} \ (\mu_r H_m + 2 w - B_m),$$

where μ_r is the initial slope of either curve, and the upper sign is used for the upper curve, and vice versa.

The above curve has an inflection point whose location depends upon the curve parameters w, μ_r, H_m, and B_m. Fitting the inflection point would generally require a fifth coefficient, and therefore a fourth degree polynomial.

When the cubic fit to actual data was attempted, the derived equation was not monotonic. Therefore, this function was abandoned. The cubic function might be good for moderate flux densities.

4-50

4.3.3.3 Hyperbolic Tangent Function

The hyperbolic tangent functions considered were of the form,

$$B = A_1 + A_2 \tanh A_3 (H + A_4)$$

Such functions have this distinct disadvantage of being symmetrical about the inflection point $H = -A_4$, $B = A_1$. Generally, no such symmetry exists in physical curves. The use of multiples of the argument or powers of the hyperbolic tangent function will make the curve unsymmetrical, but at the cost of considerable complexity. The use of two different sets of coefficients, A_i, for the portions of the curve above and below the inflection point will also make the curve unsymmetrical. However, it was felt that piecewise continuous functions are undesirable and to be used only as a last resort. If they are used, simpler functions than the hyperbolic tangent should prove to be satisfactory. All of these considerations led to the abandonment of the hyperbolic tangent function.

4.3.3.4 Inverse Tangent Function

The inverse tangent function attempted was of the form,

$$\frac{B}{B_m} = \frac{\tan^{-1}\left(K \sin \frac{\pi H}{2H_m}\right)}{\tan^{-1} K} \, .$$

This yielded a poor fit to an actual curve, in the vicinity of the inflection point. The fit to actual data required a trial and error process. Furthermore, the function is symmetrical about its inflection point, thus suffering from all of the shortcomings of the hyperbolic tangent function. For these reasons, this function was abandoned.

4.3.3.5 Froelich's Equation

Froelich's equation was presented in Reference 3, and is discussed briefly in Reference 4. The equation is

$$B = \frac{aH}{b+H} \, .$$

The coefficients a and b were fitted to one of the Allegheny Ludlum curves. The two end points were used to determine the coefficients. Then the midway point was tested, but the error was more than ten percent. Therefore, this form was abandoned. The form is inherently limited to either concave downward or concave upward curves. Therefore, at best, the use of this form would result in a piecewise continuous function. Furthermore, care would have to be exercised that the denominator did not become infinite within the H range used.

4.3.3.6 First Modification of Froelich's Equation

The expression considered is

$$B = \frac{a(H \pm H_c)}{H + b} \, ,$$

where H_c is the coercive force. The plus sign is used for the upper curve, and the minus sign for the lower curve.

If $\underline{a}$ and $\underline{b}$ are chosen to make the upper curve pass through the points corresponding to the residual flux density, $(0, B_r)$, the coercive force, $(-H_c, 0)$, and the positive maximum, (H_m, B_m), then

$$\frac{a}{b} = \frac{B_r}{H_c} ,$$

and

$$\frac{B}{B_m} = \frac{\dfrac{B_r}{B_m}\left(\dfrac{H + H_c}{H_m}\right)}{\dfrac{H_c}{H_m}\left(1 - \dfrac{H}{H_m}\right) + \dfrac{B_r}{B_m} \cdot \dfrac{H}{H_m}\left(1 + \dfrac{H_c}{H_m}\right)} .$$

Unfortunately, when $H = -H_m$ is substituted into this expression, the result is $B \approx +B_m$, for H_c considerably less than H_m. Evidently, this form is also limited as to the range of H, and would necessitate the use of piecewise continuous functions. Therefore, it was abandoned.

4.3.3.7 Second Modification of Froelich's Equation

The near successes obtained with forms similar to Froelich's equation led to further attempts with similar expressions. The following expression uses a quadratic denominator to better fit the curve shape:

$$B = C_4 + \frac{C_3}{1 + C_1 H + C_2 H^2} .$$

This expression was fitted to most of the Allegheny Ludlum curves by means of an IBM 7094 digital computer program. The program solved for the coefficients from four input BH points, recalculated these points to determine that the errors in fitting were only small errors due to roundoff, calculated B for three interpolated and two extrapolated values of H, and printed out the real zeroes of the denominator or indicated that these were complex numbers. When the zeroes are real, there is an infinite discontinuity in the BH curve. When the zeroes are complex, there is a finite peak in the curve. If either the peak or the discontinuity occurs within the range of H for the curve being fitted, the expression is useless. Unfortunately, this was the case for a considerable number of the Allegheny Ludlum curves. Therefore, this functional form had to be abandoned, in spite of the considerable effort that had been expended on it.

APPENDIX I.
EDDY-CURRENT LOSSES IN RODS

It will be shown that the torque due to eddy currents in the magnetic rods is negligible in comparison with that due to hysteresis. Since the effect is to be shown negligible, a simplified worst-case analysis is sufficient.

Assume that one rod is rotating at angular velocity ω in a uniform magnetic field, H_m, in such a way that the rod lines up with the field at two instants during one revolution. The flux density when so aligned is B_m. Assuming a linear relation between H and B as a gross approximation, the flux density in the rod is

$$B = B_m \sin \omega t. \tag{I-1}$$

Its time derivative is

$$\dot{B} = \omega B_m \cos \omega t. \tag{I-2}$$

The changing flux in the rod induces eddy currents. These, in turn, cause a torque which opposes the motion which caused the change in the first place, in accordance with Lenz's Law. It is easily shown that the torque is

$$T = \frac{\pi R^4 L \dot{B}^2}{8 \rho \omega}, \tag{I-3}$$

where R is the radius, L is the length, and ρ is the electrical resistivity of the rod. From Equations (I-1) and (I-2), the peak torque is

$$T_P = \frac{\pi R^4 L \omega B_m^2}{8 \rho}. \tag{I-4}$$

For the rods used, R is 0.14 cm., L is 152.5 cm., and ρ is 50,000 abohm-cm. It will be assumed that ω is twice the orbital angular velocity, or 0.00203 radians per second. The peak flux density, B_m, is 9,200 gauss. The peak torque is then 0.080 dyne-centimeters per rod.

The peak value of the hysteresis torque is calculated for comparison. The magnetic moment of one rod is

$$M = \frac{0.73}{4\pi} V B_c = \frac{0.73 R^2 L}{4} B_c, \tag{I-5}$$

where V is the volume of the rod, and B_c is the flux density at the center. The factor 0.73 accounts for the effect of the gradual reduction of flux from the center to each end of the rod. For the rods used, which have a peak flux density of 9,200 gauss, the peak value of the magnetic moment of one rod is 5,020 dyne-centimeters per oersted. This occurs for an applied field of 0.592 oersted. The peak torque is therefore 2,980 dyne-centimeters. This is more than four orders of magnitude greater than the peak value of the eddy-current torque. Therefore, the latter is negligible.

APPENDIX II.
PROGRAM FOR FITTING SEVENTH-DEGREE POLYNOMIAL

An IBM 7094 digital computer program was used to derive a least-squares, seventh-degree polynomial for each of the reference BH curves. The program will (1) accept raw data, that is, values of flux density and internal field of a ring sample; (2) convert to the external field applied to a rod; (3) shift the data to an arbitrary origin; (4) solve the least-squares equations; (5) substitute each abscissa back into the derived polynomial and evaluate it; (6) compute the error in the fit at each such point; and (7) printout all of these results. The polynomial is forced to go through the point $(0, 0)$ by omitting the constant term from the general expression.

The input data are values of H and B. Assume that N pairs are given:

$$
\begin{aligned}
&H_1 \quad B_1, \\
&H_j \quad B_j, \\
&H_N \quad B_N.
\end{aligned}
\tag{II-1}
$$

Two factors are also used. The first is the ascending-descending index, D_A, which is $+1$ for an ascending curve and -1 for a descending curve. The polynomial fit is for an ascending curve starting at $(0, 0)$. If the curve is descending, the algebraic signs of all of the data values are reversed.

The second factor is the demagnetization factor, D_M. This is used to determine the external field of a rod corresponding to the internal field of a ring sample. It is assumed that the latter is input, and the former is then computed. In case the input is the external field, the factor D_M is simply set equal to zero.

The external field value is computed for each data point,

$$
\begin{aligned}
&H_{E1} = H_1 + D_M B_1, \\
&H_{Ej} = H_j + D_M B_j, \\
&H_{EN} = H_N + D_M B_N.
\end{aligned}
\tag{II-2}
$$

The increments for translating the first point to $(0, 0)$ are computed. For the field,

$$
D_H = - D_A H_{E1}.
\tag{II-3}
$$

For the flux density,

$$
D_B = - D_A B_1.
\tag{II-4}
$$

These increments are applied to all of the input data. For the field,

$$H_{S2} = D_H + D_A H_{E2},$$

$$H_{Sj} = D_H + D_A H_{Ej},$$

$$H_{SN} = D_H + D_A H_{EN}.$$

$$(II-5)$$

For the flux density,

$$B_{S2} = D_B + D_A B_2,$$

$$B_{Sj} = D_B + D_A B_j,$$

$$B_{SN} = D_B + D_A B_N.$$

$$(II-6)$$

The $(H_{S2}, B_{S2}) \ldots \ldots (H_{SN}, B_{SN})$ constitute N-1 pairs of data to be used to fit the polynomial,

$$B_S = A_1 H_S + A_2 H_S^2 + \ldots \ldots + A_7 H_S^7,$$

$$(II-7)$$

by the method of least squares. The equations for the coefficients are

$$A_1 \sum_j H_{Sj}^2 + A_2 \sum_j H_{Sj}^3 + A_3 \sum_j H_{Sj}^4 + A_4 \sum_j H_{Sj}^5 + A_5 \sum_j H_{Sj}^6 + A_6 \sum_j H_{Sj}^7 + A_7 \sum_j H_{Sj}^8 = \sum_j B_{Sj} H_{Sj}^1,$$

$$A_1 \sum_j H_{Sj}^3 + A_2 \sum_j H_{Sj}^4 + A_3 \sum_j H_{Sj}^5 + A_4 \sum_j H_{Sj}^6 + A_5 \sum_j H_{Sj}^7 + A_6 \sum_j H_{Sj}^8 + A_7 \sum_j H_{Sj}^9 = \sum_j B_{Sj} H_{Sj}^2,$$

$$A_1 \sum_j H_{Sj}^4 + A_2 \sum_j H_{Sj}^5 + A_3 \sum_j H_{Sj}^6 + A_4 \sum_j H_{Sj}^7 + A_5 \sum_j H_{Sj}^8 + A_6 \sum_j H_{Sj}^9 + A_7 \sum_j H_{Sj}^{10} = \sum_j B_{Sj} H_{Sj}^3,$$

$$A_1 \sum_j H_{Sj}^5 + A_2 \sum_j H_{Sj}^6 + A_3 \sum_j H_{Sj}^7 + A_4 \sum_j H_{Sj}^8 + A_5 \sum_j H_{Sj}^9 + A_6 \sum_j H_{Sj}^{10} + A_7 \sum_j H_{Sj}^{11} = \sum_j B_{Sj} H_{Sj}^4,$$

$$A_1 \sum_j H_{Sj}^6 + A_2 \sum_j H_{Sj}^7 + A_3 \sum_j H_{Sj}^8 + A_4 \sum_j H_{Sj}^9 + A_5 \sum_j H_{Sj}^{10} + A_6 \sum_j H_{Sj}^{11} + A_7 \sum_j H_{Sj}^{12} = \sum_j B_{Sj} H_{Sj}^5,$$

$$A_1 \sum_j H_{Sj}^7 + A_2 \sum_j H_{Sj}^8 + A_3 \sum_j H_{Sj}^9 + A_4 \sum_j H_{Sj}^{10} + A_5 \sum_j H_{Sj}^{11} + A_6 \sum_j H_{Sj}^{12} + A_7 \sum_j H_{Sj}^{13} = \sum_j B_{Sj} H_{Sj}^6,$$

$$A_1 \sum_j H_{Sj}^8 + A_2 \sum_j H_{Sj}^9 + A_3 \sum_j H_{Sj}^{10} + A_4 \sum_j H_{Sj}^{11} + A_5 \sum_j H_{Sj}^{12} + A_6 \sum_j H_{Sj}^{13} + A_7 \sum_j H_{Sj}^{14} = \sum_j B_{Sj} H_{Sj}^7,$$

$$(II-8)$$

where j runs from 2 to N.

These are solved for the coefficients, A_i, by a subroutine used for simultaneous, linear equations.

Each abscissa, H_{Sj}, is substituted in turn into Equation (II-7) and the corresponding value of flux density, B_{Cj}, is computed,

$$B_{C2} = A_1 H_{S2} + A_2 H_{S2}^2 + \ldots + A_7 H_{S2}^7,$$
$$\text{--}$$
$$B_{Cj} = A_1 H_{Sj} + A_2 H_{Sj}^2 + \ldots + A_7 H_{Sj}^7,$$
$$\text{--}$$
$$B_{CN} = A_1 H_{SN} + A_2 H_{SN}^2 + \ldots + A_7 H_{SN}^7. \qquad \text{(II-9)}$$

The error in the polynomial at each point is computed. It is the difference between the flux density computed from the polynomial and the corresponding input value,

$$B_{E2} = B_{C2} - B_{S2},$$
$$\text{------------------}$$
$$B_{Ej} = B_{Cj} - B_{Sj},$$
$$\text{------------------}$$
$$B_{EN} = B_{CN} - B_{SN}. \qquad \text{(II-10)}$$

The computed values of the flux density are retranslated, by subtracting D_B,

$$B_{R1} = -D_B,$$
$$B_{R2} = B_{C2} - D_B,$$
$$\text{------------------}$$
$$B_{Rj} = B_{Cj} - D_B,$$
$$\text{------------------}$$
$$B_{RN} = B_{CN} - D_B. \qquad \text{(II-11)}$$

The argument of the fitted polynomial remains the translated value of the field, which is zero at the beginning point of the curve. This is the same way that the polynomial is used in the main program.

It should be emphasized that the fitted polynomial pertains to an ascending curve.

APPENDIX III.
ELEVEN-POINT FIT OF THE RATIONAL FRACTION

This appendix lists the equations, input, and output of an IBM 7094 program used for deriving the coefficients, A_i, of the function

$$B = \sum_i \frac{A_i}{(H-H_i)^2 + C^2} \; . \tag{III-1}$$

This function may be used as an analytical approximation for a BH curve, as discussed in Section 4.3.2.1.

The range of H is divided by 20, to obtain 21 points. The corresponding 21 values of B, from the curve to be fitted, are also tabulated. The eleven alternate pairs of values, beginning with the first pair, are used for fitting. The intermediate ten pairs of values are used for checking the goodness of the fit.

A rearrangement of Equation (III-1) is convenient. First, the increment between consecutive values of H (1/20 of the range) is designated ΔH. Also, C is expressed as a multiplier, H_K, times ΔH. Then

$$B(\Delta H)^2 = \sum_i \frac{A_i}{n^2 + H_K^2} \; , \tag{III-2}$$

where n is zero or a positive integer. The method of summing is explained later.

The program may be used for fitting either ascending or descending magnetic hysteresis curves. An index, D_A, is set equal to +1 if the curve is ascending and -1 if it is descending.

The input to the program consists of the D_A index, the multiplier, H_K, and the 21 pairs of values:

$$H_0, \; B_0,$$
$$H_1, \; B_1,$$
$$\ldots \ldots$$
$$H_{20}, \; B_{20}. \tag{III-3}$$

The first computations are all of the denominator factors which will be required. These are for

$$n = 0, \; 1, \; 2, \; \ldots \ldots \; 20. \tag{III-4}$$

The factors are

$$R_0 = \frac{1}{H_K{}^2} ,$$

$$R_1 = \frac{1}{1^2 + H_K{}^2} ,$$

$$R_2 = \frac{1}{2^2 + H_K{}^2} ,$$

$$\cdots\cdots\cdots\cdots$$

$$R_{20} = \frac{1}{20^2 + H_K{}^2} . \qquad\qquad\text{(III-5)}$$

The coordinates of the eleven points to be fitted are substituted into Equation (III-2). For any general point, one of the terms will correspond to n = 0, the two adjacent terms will correspond to n = 1, etc. The scheme is apparent from an examination of the subscripts in the determinant of the system of equations. Since alternate points are used, only R factors with even subscripts appear. The eleven simultaneous linear equations for the A_i are, in matrix form:

$$
\begin{bmatrix}
R_0 & R_2 & R_4 & R_6 & R_8 & R_{10} & R_{12} & R_{14} & R_{16} & R_{18} & R_{20} \\
R_2 & R_0 & R_2 & R_4 & R_6 & R_8 & R_{10} & R_{12} & R_{14} & R_{16} & R_{18} \\
R_4 & R_2 & R_0 & R_2 & R_4 & R_6 & R_8 & R_{10} & R_{12} & R_{14} & R_{16} \\
R_6 & R_4 & R_2 & R_0 & R_2 & R_4 & R_6 & R_8 & R_{10} & R_{12} & R_{14} \\
R_8 & R_6 & R_4 & R_2 & R_0 & R_2 & R_4 & R_6 & R_8 & R_{10} & R_{12} \\
R_{10} & R_8 & R_6 & R_4 & R_2 & R_0 & R_2 & R_4 & R_6 & R_8 & R_{10} \\
R_{12} & R_{10} & R_8 & R_6 & R_4 & R_2 & R_0 & R_2 & R_4 & R_6 & R_8 \\
R_{14} & R_{12} & R_{10} & R_8 & R_6 & R_4 & R_2 & R_0 & R_2 & R_4 & R_6 \\
R_{16} & R_{14} & R_{12} & R_{10} & R_8 & R_6 & R_4 & R_2 & R_0 & R_2 & R_4 \\
R_{18} & R_{16} & R_{14} & R_{12} & R_{10} & R_8 & R_6 & R_4 & R_2 & R_0 & R_2 \\
R_{20} & R_{18} & R_{16} & R_{14} & R_{12} & R_{10} & R_8 & R_6 & R_4 & R_2 & R_0
\end{bmatrix}
\begin{bmatrix}
A_0 \\ A_1 \\ A_2 \\ A_3 \\ A_4 \\ A_5 \\ A_6 \\ A_7 \\ A_8 \\ A_9 \\ A_{10}
\end{bmatrix}
= D_A (\Delta H)^2
\begin{bmatrix}
B_0 \\ B_2 \\ B_4 \\ B_6 \\ B_8 \\ B_{10} \\ B_{12} \\ B_{14} \\ B_{16} \\ B_{18} \\ B_{20}
\end{bmatrix}
$$

$$\text{(III-6)}$$

After solving for the eleven A_i, the computed and the intermediate points are tested, using Equation (III-2) solved for B. The values of B so computed are designated B_C. The twenty-one B_C's are computed from the following equations:

$$B_{C0} = \frac{D_A}{(\Delta H)^2} (R_0 A_0 + R_2 A_1 + R_4 A_2 + R_6 A_3 + R_8 A_4 + R_{10} A_5 + R_{12} A_6$$
$$+ R_{14} A_7 + R_{16} A_8 + R_{18} A_9 + R_{20} A_{10}),$$

$$B_{C1} = \frac{D_A}{(\Delta H)^2} (R_1 A_0 + R_1 A_1 + R_3 A_2 + R_5 A_3 + R_7 A_4 + R_9 A_5 + R_{11} A_6$$
$$+ R_{13} A_7 + R_{15} A_8 + R_{17} A_9 + R_{19} A_{10}),$$

$$B_{C2} = \frac{D_A}{(\Delta H)^2} (R_2 A_0 + R_0 A_1 + R_2 A_2 + R_4 A_3 + R_6 A_4 + R_8 A_5$$
$$+ R_{10} A_6 + R_{12} A_7 + R_{14} A_8 + R_{16} A_9 + R_{18} A_{10}),$$

$$B_{C3} = \frac{D_A}{(\Delta H)^2} (R_3 A_0 + R_1 A_1 + R_1 A_2 + R_3 A_3 + R_5 A_4 + R_7 A_5$$
$$+ R_9 A_6 + R_{11} A_7 + R_{13} A_8 + R_{15} A_9 + R_{17} A_{10}),$$

$$B_{C4} = \frac{D_A}{(\Delta H)^2} (R_4 A_0 + R_2 A_1 + R_0 A_2 + R_2 A_3 + R_4 A_4 + R_6 A_5$$
$$+ R_8 A_6 + R_{10} A_7 + R_{12} A_8 + R_{14} A_9 + R_{16} A_{10}),$$

$$B_{C5} = \frac{D_A}{(\Delta H)^2} (R_5 A_0 + R_3 A_1 + R_1 A_2 + R_1 A_3 + R_3 A_4 + R_5 A_5$$
$$+ R_7 A_6 + R_9 A_7 + R_{11} A_8 + R_{13} A_9 + R_{15} A_{10}),$$

$$B_{C6} = \frac{D_A}{(\Delta H)^2} (R_6 A_0 + R_4 A_1 + R_2 A_2 + R_0 A_3 + R_2 A_4 + R_4 A_5$$
$$+ R_6 A_6 + R_8 A_7 + R_{10} A_8 + R_{12} A_9 + R_{14} A_{10}),$$

$$B_{C7} \quad \frac{D_A}{(\Delta H)^2} (R_7 A_0 + R_5 A_1 + R_3 A_2 + R_1 A_3 + R_1 A_4 + R_3 A_5$$
$$+ R_5 A_6 + R_7 A_7 + R_9 A_8 + R_{11} A_9 + R_{13} A_{10}),$$

$$B_{C8} = \frac{D_A}{(\Delta H)^2} (R_8 A_0 + R_6 A_1 + R_4 A_2 + R_2 A_3 + R_0 A_4 + R_2 A_5$$
$$+ R_4 A_6 + R_6 A_7 + R_8 A_8 + R_{10} A_9 + R_{12} A_{10}),$$

$$B_{C9} = \frac{D_A}{(\Delta H)^2} (R_9 A_0 + R_7 A_1 + R_5 A_2 + R_3 A_3 + R_1 A_4 + R_1 A_5$$
$$+ R_3 A_6 + R_5 A_7 + R_7 A_8 + R_9 A_9 + R_{11} A_{10}),$$

$$B_{C10} = \frac{D_A}{(\Delta H)^2} (R_{10}A_o + R_8A_1 + R_6A_2 + R_4A_3 + R_2A_4 + R_oA_5$$
$$+ R_2A_6 + R_4A_7 + R_6A_8 + R_8A_9 + R_{10}A_{10}),$$

$$B_{C11} = \frac{D_A}{(\Delta H)^2} (R_{11}A_o + R_9A_1 + R_7A_2 + R_5A_3 + R_3A_4 + R_1A_5$$
$$+ R_1A_6 + R_3A_7 + R_5A_8 + R_7A_9 + R_9A_{10}),$$

$$B_{C12} = \frac{D_A}{(\Delta H)^2} (R_{12}A_o + R_{10}A_1 + R_8A_2 + R_6A_3 + R_4A_4 + R_2A_5$$
$$+ R_oA_6 + R_2A_7 + R_4A_8 + R_6A_9 + R_8A_{10}),$$

$$B_{C13} = \frac{D_A}{(\Delta H)^2} (R_{13}A_o + R_{11}A_1 + R_9A_2 + R_7A_3 + R_5A_4 + R_3A_5$$
$$+ R_1A_6 + R_1A_7 + R_3A_8 + R_5A_9 + R_7A_{10}),$$

$$B_{C14} = \frac{D_A}{(\Delta H)^2} (R_{14}A_o + R_{12}A_1 + R_{10}A_2 + R_8A_3 + R_6A_4 + R_4A_5$$
$$+ R_2A_6 + R_oA_7 + R_2A_8 + R_4A_9 + R_6A_{10}),$$

$$B_{C15} = \frac{D_A}{(\Delta H)^2} (R_{15}A_o + R_{13}A_1 + R_{11}A_2 + R_9A_3 + R_7A_4 + R_5A_5$$
$$+ R_3A_6 + R_1A_7 + R_1A_8 + R_3A_9 + R_5A_{10}),$$

$$B_{C16} = \frac{D_A}{(\Delta H)^2} (R_{16}A_o + R_{14}A_1 + R_{12}A_2 + R_{10}A_3 + R_8A_4 + R_6A_5$$
$$+ R_4A_6 + R_2A_7 + R_oA_8 + R_2A_9 + R_4A_{10}),$$

$$B_{C17} = \frac{D_A}{(\Delta H)^2} (R_{17}A_o + R_{15}A_1 + R_{13}A_2 + R_{11}A_3 + R_9A_4 + R_7A_5$$
$$+ R_5A_6 + R_3A_7 + R_1A_8 + R_1A_9 + R_3A_{10}),$$

$$B_{C18} = \frac{D_A}{(\Delta H)^2} (R_{18}A_o + R_{16}A_1 + R_{14}A_2 + R_{12}A_3 + R_{10}A_4 + R_8A_5$$
$$+ R_6A_6 + R_4A_7 + R_2A_8 + R_oA_9 + R_2A_{10}),$$

$$B_{C19} = \frac{D_A}{(\Delta H)^2} (R_{19}A_o + R_{17}A_1 + R_{15}A_2 + R_{13}A_3 + R_{11}A_4 + R_9A_5$$
$$+ R_7A_6 + R_5A_7 + R_3A_8 + R_1A_9 + R_1A_{10}),$$

$$B_{C20} = \frac{D_A}{(\Delta H)^2} (R_{20}A_0 + R_{18}A_1 + R_{16}A_2 + R_{14}A_3 + R_{12}A_4 + R_{10}A_5$$

$$+ R_8A_6 + R_6A_7 + R_4A_8 + R_2A_9 + R_0A_{10}). \tag{III-7}$$

The error in each computed value is the difference between that value and the actual (input) value of B. These errors are computed from

$$B_{E0} = B_{C0} - \ ,$$

$$B_{E1} = B_{C1} - B_1,$$

$$B_{E2} = B_{C2} - B_2,$$

$$\dots\dots\dots\dots$$

$$B_{E20} = B_{C20} - B_{20}. \tag{III-8}$$

The output includes the eleven coefficients, A_0, A_1, A_2, ... A_{10}, and the tabulated input pairs of values, computed flux density, and error in flux density:

H_0	B_0	B_{C0}	B_{E0}
H_1	B_1	B_{C1}	B_{E1}
H_2	B_2	B_{C2}	B_{E2}
H_{20}	B_{20}	B_{C20}	$B_{E20}.$

REFERENCES

1. Hinrichs, R. H. ,"Attitude Dynamics of an N-Rod Satellite, GE Spacecraft Department Report 64SD5276, 30 December 1964.

2. Bozorth, R. M. , "Ferromagnetism," D. Van Nostrand Co. Inc., New York, 1951.

3. Froelich, O. , "Handbuch der Elektricitaet und des Magnetismus," 1886.

4. Timbie, W. H. , and Bush, V. , "Principles of Electrical Engineering," John Wiley and Sons, Inc. , New York, 1922.